Physics – Uspekhi **41** (8) 735 – 759 (1998)

REVIEWS OF TOPICAL PROBLEMS PACS numbers: **71.20.–b**, **71.55.–i**, **74.70.–b**, **78.90.+t**

Thallium dopant in lead chalcogenides: investigation methods and peculiarities

S A Nemov, Yu I Ravich

Contents

Abstract. The body of experimental and theoretical data on transport phenomena, optical absorption, low-temperature heat capacity, tunnelling spectroscopy, magnetic susceptibility, superconductivity, and self-compensation are summarized for thallium-doped lead chalcogenides Pb*M* (*M* = Te, Se, S) and Pb*M*-based solid solutions. The physical properties of the semiconducting compounds are explained in a unified manner using the concept of resonance Tl states located in the valence band of the compound. The basic parameters of resonance impurity states are estimated and their dependences on temperature, pressure and material composition are determined.

1. Introduction

— *Thallium is an exceptional acceptor impurity*.
— *Exceptionally different*.
(Paraphrase of a TV catchphrase)

The search for and investigation of impurity states produced by group III elements of the periodic table in IV – VI compound semiconductors started after Kaidanov and coworkers discovered resonance indium states in the conduction band of lead telluride in the early 70s. These states possessed many interesting properties. First and foremost, the pinning (stabilization) of the Fermi level was discovered, which is responsible, in particular, for the extraordinary high spatial homogeneity of the samples in the concentration of charge carriers [1 – 4]. This situation existed despite the presence of a great amount of impurities not quite uniformly distributed over the samples. The location of the Fermi level is readily determined by the energy of resonance (quasi-local) states, which proves to be dependent on the crystal temperature, pressure, and composition. The discovery of indium impurity states has opened up new ways for controlling the properties of IV – VI compounds and their operational features. Therefore, the exploration and sophisticated study of impurity states produced by other dopants (including thallium) in IV – VI semiconductors was found vital from both the scientific and practical standpoints.

Whereas indium as a donor exerts a limited action on PbTe, thallium shows evidence of being a deep acceptor in lead chalcogenides. It was originally expected that both thallium and indium should produce resonance levels that stabilize the chemical potential in the valence band, rather than in the conduction band. Such levels really were discovered [5 – 8], however the reality turned out richer and more diverse than preliminary expectations. In spite of sharing some common features, the thallium and indium impurity states showed significant differences and each of the two property aggregates was found unique in its own way.

S A Nemov, Yu I Ravich Radiophysics Department,
St. Petersburg State Technical University,
ul. Politekhnicheskaya 29, 195251 St. Petersburg, Russia
Tel. (812) 552 96 71
E-mail: nemov@twonet.stu.neva.ru; ravich@twonet.stu.neva.ru

Received 1 September 1997, revised 16 February 1998
Uspekhi Fizicheskikh Nauk **168** (8) 817 – 842 (1998)
Translated by A A Radzig; edited by S N Gorin

Long-term relaxation of the electron nonequilibrium distribution with typical times of up to several hours, which was observed at low (liquid-helium) temperatures, stands out among the peculiarities of indium-doped lead chalcogenides [9, 10]. This relaxation was accounted for by the crystal lattice rearrangement in the vicinity of an impurity atom upon changing the impurity charge state. In particular, Volkov, Osipov and Pankratov [11, 12] developed a theory based on the assumption that an indium dopant in PbTe makes a Jahn – Teller center. The effective attraction of two impurity-localized electrons to one another, which was suggested in Refs [13 – 15], may be related directly to the lattice rearrangement. In other words, electrons in the indium-atom-localized state are described by the model of centers with a negative correlation Hubbard energy originally adopted by Anderson [16] for the case of amorphous semiconductors. For a large content of In impurity (3 – 20 at.%), the hopping conductivity over localized states was examined [17, 18]. Based on the analysis of the In-concentration-dependent hopping conductivity, Ravich, Nemov and Proshin [19] demonstrated that the impurity wave function localization radius is very small (around 6 A).

Neither long-term relaxation, nor a negative Hubbard energy and hopping conductivity were observed in lead chalcogenides upon thallium doping. But on the other hand, a large variety of other phenomena were found, which were no less dramatic and frequently unexpected at the moment of discovery. It is appropriate at this point to think back to the superconductivity of semiconductors with an exceptionally high critical temperature, resonance scattering of holes, low-temperature heat capacity (conditioned by the thallium resonance states), resistance anomalies (having analogy to the Kondo effect), and, finally, strong self-compensation for the thallium acceptor action by intrinsic crystal-lattice defects. The current review is devoted to the experimental investigation of these effects.

2. Transport phenomena in thallium-doped lead chalcogenides

2.1 Electron spectra of IV – VI compound semiconductors

We preface presenting results of the investigation of thallium-impurity states with a brief look at the properties of IV – VI compound semiconductors that are essential to the problem of impurity states. Our main concern in the following sections is with peculiarities of the lead chalcogenide band structure. For an extended discussion of lead chalcogenide properties, the reader can familiarize himself with the book [20] and a series of review articles, for instance, Ref. [21].

Lead chalcogenides crystallize in the NaCl-type structure characteristic of ionic crystals. In this case, the nature of chemical bonding is rather complicated, approximating to an ionic-covalent-metallic bond [22]. If the bond, in an effort to simplify the problem, is conceived as poorly ionic, then it may be suggested that a bivalent atom of lead loses two electrons to a bond with chalcogen atoms and remains in the form of a Pb^{+2} ion, while the chalcogen atoms bear a double negative charge. The ionic character of the lattice manifests itself in a sizable (by an order of magnitude) difference between static ε_0 and high-frequency ε_∞ permittivities (see Table 1). The large value of ε_0 exhibits a strong dependence on temperature [by the $(T - T_c)^{-1}$ law with $T_c < 0$ K] and charge carrier concentration (the table includes results of several measurements only). The magnitude and temperature dependence of ε_0 give evidence of the proximity of the phase state of lead chalcogenides to a ferroelectric transition, which occurs in SnTe, GeTe and their solid solutions with lead chalcogenides. The difference in the magnitudes of ε_0 and ε_∞ is raised from distinctions between the frequencies of longitudinal and transverse optical phonons along with the existence of a soft transverse mode.

Table 1. Some parameters of lead chalcogenides.

Parameter	PbTe	PbSe	PbS
ε_g, eV ($T = 0$ K)	0.187	0.145	0.283
$\Delta\varepsilon_v$, eV ($T = 0$ K)	0.17	~ 0.3	$\geqslant 0.3$
$m^*_{\parallel p}/m_0$	0.31	0.068	0.105
$m^*_{\perp p}/m_0$	0.022	0.034	0.075
$m^*_{\parallel n}/m_0$	0.24	0.070	0.105
$m^*_{\perp n}/m_0$	0.024	0.040	0.080
u_p, cm^2/V s ($T = 300$ K)	840	1000	620
u_n, cm^2/V s ($T = 300$ K)	1730	1000	610
ε_0 ($T = 300$ K)	414	204	169
ε_∞	33	23	17

Note: There is a significant scatter in the magnitudes obtained by different researchers using a variety of techniques. The table lists typical values covered by the monograph [20] and the reference book [22].

The band parameters of lead chalcogenides are qualitatively close. The energy gap ε_g is relatively small in all three compounds (see Table 1). This gap is restricted by the main extrema of the electron and hole bands, which are located at the point L of the Brillouin zone. Direct optical transitions are allowed near the intrinsic absorption edge. The above properties lead to an almost mirror character for the electron dispersion laws near the edges of the electron and hole bands, small magnitudes of the effective masses, and strong Kane-type non-parabolicity.

With the inversion center of the lattice placed at a lead site, the Bloch amplitudes of electron wave functions in the conduction band minima constitute odd functions of L_6^- symmetry, whereas they are even functions of L_6^+ symmetry in the valence band maxima. The electron wave functions in the valence band may be constructed predominantly from chalcogen p functions, whilst those in the conduction band from lead p functions [23 – 25]; the energy levels of s electrons in lead and chalcogen lie well below the chalcogen valence p bands. Near the extrema, the isoenergetic surfaces make up ellipsoids of revolution, which are extended in the $\langle 111 \rangle$ directions; the anisotropy of the effective masses falls from ~ 10 to ~ 1 along the PbTe – PbSe – PbS row.

There is a second maximum at the Σ point (see Fig. 1) in addition to the primary L extremum of the valence band. The energy separation between the two maxima in the valence band takes its smallest value in PbTe ($\Delta\varepsilon_v = 0.17$ eV for $T = 0$ K). The width of the forbidden band ε_g increases in all three lead chalcogenides, viz., $\partial\varepsilon_g/\partial T \approx 4 \times 10^{-4}$ eV K^{-1} for $T > 50$ K, with a rise in temperature, whereas the spacing between the two valence band maxima reduces at approximately the same rate. At a temperature of about 450 K, the Σ extremum in PbTe has the same energy as the L extremum; at higher temperatures, the valence band edge is defined by the Σ maximum and the energy gap becomes indirect and temperature-independent. The energy separation between valence subbands in PbSe and PbS is much wider than in PbTe and the additional maximum is always lower than the L maximum.

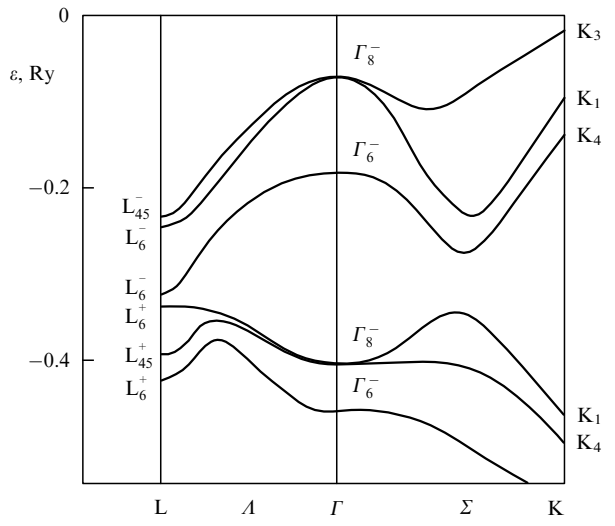

Figure 1. Energy spectrum of PbTe in the vicinity of the forbidden band [20].

With a rise in pressure, the forbidden band width reduces in all three lead chalcogenides, viz., $\partial\varepsilon_g/\partial P \approx -8 \times 10^{-6}$ eV bar^{-1}; in this case, the energy separation between valence subbands grows, i.e., the influence of pressure is equivalent to lowering of the temperature.

On substitution of tin atoms for lead in PbTe and PbSe, the energy gap ε_g also gets narrower, so that a gapless state is reached in solid solutions of $Pb_{1-x}Sn_xTe$ and $Pb_{1-x}Sn_xSe$ with increasing x. Then, an inversion of extrema takes place, and the main extremum of the conduction band in solid solutions with a rich content of Sn corresponds to an L_6^+-type symmetry, while that of the valence band to an L_6^--type symmetry.

Upon variations of temperature, pressure and solid-solution composition, the effective masses vary approximately proportionally to ε_g in the vicinity of L extrema, which causes, in particular, a prominent temperature dependence of effective masses.

At temperatures above ~ 50 K, electron and hole scattering from acoustic phonons and their polar scattering from optical phonons are considered as the main scattering mechanisms [26]. It seems likely that the part of scattering ascribed to acoustic phonons is really governed by a nonpolar interaction with optical phonons and intervalley transitions. At low temperatures, weak scattering by impurity atoms and defects prevails and the mobility of carriers exceeds 10^6 cm^2 (V s)$^{-1}$.

The IV – VI compounds crystallize with wide deviations from stoichiometry and this circumstance is responsible for the presence of a large number (routinely of order 10^{18} – 10^{19} cm^{-3}) of electrically active intrinsic defects (for example, vacancies) in the metal or chalcogen sublattices. From theoretical expectations and electrophysical data it follows that a lead vacancy (an excess chalcogen atom) yields two holes, while a chalcogen vacancy (an excess lead) yields two electrons. Electrically active doping is also effected by both donor (halogens, In, Ga, Bi, etc.) and acceptor (alkali metals, Tl, etc.) impurities.

Owing to the high dielectric constant of the IV – VI compounds and low effective masses of charge carriers in them, the Coulomb potential of impurities and vacancies does not produce shallow hydrogen-like impurity levels at high concentrations of impurities and intrinsic defects, but deep and resonance states may arise through the non-Coulomb part of the impurity potential. As mentioned in the introduction, quasi-local levels are brought about in the lead chalcogenide conduction band on doping IV – VI compounds with In [1 – 3], which lie 0.07 eV above the bottom of the conduction band in PbTe at $T = 4$ K. They are nearing the edge of the energy gap with a rise in temperature and then end up as local levels in the gap. At low temperatures, substitution of tin for Pb atoms produces the same effect, so that the In levels in SnTe reveal themselves in the valence band and turn resonant anew.

The presence of In quasi-local levels in PbTe gives rise to pronounced pinning of the chemical potential, in particular, under additional doping with iodine which does not produce impurity levels in the forbidden energy gap. In this case the electrons transfer from iodine atoms to quasi-local In levels, during which transition the chemical potential and conduction electron concentration hardly change as long as the In band is fully filled with electrons (which occurs practically at $N_I \approx N_{In}$). Experiments on additional doping have enabled the conclusion that the impurity band capacity is two states per In atom.

The results obtained allowed Kaidanov and co-workers [1 – 3] to pose a model of lead chalcogenide doping with indium, which proved fruitful in explaining many observable properties, not only for doping with indium, but with thallium as well. In this model, the indium atom, located at a lead site in the lattice of a crystal under study, 'donates' two of its outer electrons to form a bond with the chalcogen (similar to the atom of lead), leaving one *s* electron in its place. Since the atomic *s* level of In lies significantly higher than that of Pb [27], the indium *s* electron occupies the level situated just above the conduction-band bottom and thus *s* electrons remaining at the In atom exert only weak donor effect on PbTe. Having two states per In atom, the impurity band is also capable of accepting electrons from further donors, i.e., it offers amphoteric (donor-acceptor) properties.

In the model of In quasi-local levels, the interaction energy of electrons located at the same impurity center is assumed to be negligibly small. Later on, Moĭzhes and Drabkin [14, 15] modified the above-described model and took the negative correlation energy into consideration ($U < 0$), i.e., they suggested that In in PbTe produces 'negative-U' centers. The model with $U < 0$ provides an explanation for the strong pinning of the chemical potential as well as the lack of paramagnetism and a variety of other phenomena. However, this model is more complicated, and the simplified model without electron interaction is widely used as before when interpreting experimental data, particularly for Tl, where the value of $|U|$ is evidently small.

2.2 Thallium impurity states

The greater part of our work was carried out on polycrystalline samples with grains of typical size $d \sim 0.1$ mm, which were fabricated by the powder-metallurgy method and were subjected to homogenizing annealing for 100 h at 650 °. This procedure enables fabrication of samples of lead chalcogenides and their solid solutions with electrophysical properties approaching those of single crystals.

The composition of samples and the content of thallium dopant in them were controlled using a Comibax electron microprobe, while the Li and Na impurity contents were

evaluated from their weights in the charge and composition-dependent electrophysical parameters of the samples prepared.

Investigations carried out on single crystals are considered separately in the text of the present review.

Experimentally, as noted above, thallium behaves in lead chalcogenides as an acceptor. Therefore, in the search for Tl impurity states in PbTe, it was suggested that if the thallium dopant produces resonance levels (similar to indium levels), then they need be looked for in the valence band.

When relating the impurity states of group III elements in lead chalcogenides with atomic *s* states of impurities, it seems essential that the *s* energy levels of Tl lie about 0.2 eV below those of In [27]. This also suggests that the Tl impurity states, if they occur in lead chalcogenides, lie below the In states, being conceivably located even in the valence band [3].

The complex structure of the valence band along with the involvement of two sorts of holes (with different mobilities) in energy and charge transfer evidently make the analysis of transport phenomena with the purpose of searching for resonance states deep in the valence band significantly more difficult. Therefore for gleaning more distinct information about the influence of thallium impurity on the properties of lead chalcogenides, kinetic studies began with PbSe samples [5, 28 – 30] where the supplementary extremum of the valence band is positioned well past the principal maximum as compared to PbTe. (Note that the expectations for a simpler pattern for the energy spectrum in PbSe:Tl as opposed to PbTe:Tl were not entirely realized because, as we will see below, the Tl energy levels turned out to lie deep in the valence band, near the second extremum.)

Measurements of the Hall effect demonstrated that the Hall hole concentration p at 77 K increases proportionally to N_{Tl} up to the thallium number density $N_{\mathrm{Tl}} \approx 10^{20}$ cm^{-3}, with each Tl atom generating only one hole in the valence band. This result simply depends upon the facts that Tl as an element of group III of the periodic table has one electron fewer in its outer shell than the Pb atom from group IV (replaced by thallium) and that the latter, unlike indium, does not lower the number of states in the valence band. Over the range of greater thallium concentrations, the $p(N_{\mathrm{Tl}})$ function for $T = 77$ K shows a tendency to saturation (see Fig. 2) with the limiting hole concentration, 1.2×10^{20} cm^{-3}, being several times as low as the solubility of Tl in PbTe (approximately 2 at.% for 300 °C [31]). Comparison of thallium-doped lead chalcogenides with similar materials doped instead with Na indicates that the temperature dependences of the Hall and Seebeck coefficients qualitatively hold their shapes upon thallium doping, which are conditioned by the effect of a second valence band. However, temperature dependences turn out to be markedly enhanced at the related Hall hole concentrations, the maximum of the Hall coefficient shifts to the region of lower temperatures, and its absolute value increases in PbSe and PbS, while in PbTe this value decreases.

The regularities discovered at high temperatures in PbSe:Tl were explained in terms of the thermal activation of holes to the zone of resonance states analogous to In states in PbTe but positioned deep in the valence band. In the framework of this model, a departure of the p dependence on N_{Tl} from linearity at low temperatures is related to filling of the Tl impurity band with holes. An estimate of the Tl impurity band position, made at $T = 77$ K using the limiting Hall concentration of holes, yielded a value $\varepsilon_{\mathrm{i}} \approx 0.26 \pm 0.02$ eV below the top

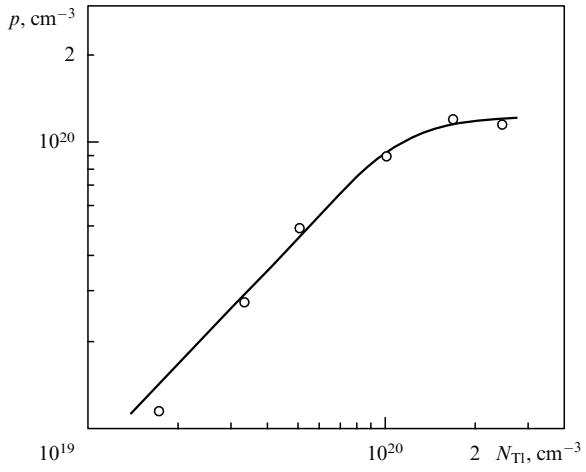

Figure 2. Maximal hole concentration (for a given thallium content) against the amount of Tl in PbSe samples at 77 K [28].

of the valence band, i.e., it lay higher than the second extremum but rather close to it.

Analysis of the temperature dependence of the Hall coefficient in samples with a thallium concentration well below the limiting one showed that the Tl impurity band position at high temperatures shifts with an increase in T toward the edge of the valence band at a rate of $\mathrm{d}\varepsilon_{\mathrm{i}}/\mathrm{d}T \approx -(1-2) \times 10^{-4}$ eV K^{-1}.

Synchronous with the above-described regularities, a distinct drop of the Hall mobility and a reduction in the absolute value of the Nernst – Ettingshausen coefficient as well as minima in the concentration dependences of the Seebeck and Nernst – Ettingshausen coefficients were observed upon PbSe doping with thallium in the neighborhood of the saturation concentration. These phenomena also testify to the contribution of thallium resonance states (see below, Section 3.1).

Experimental data similar to those discussed above were also obtained in the cases of the PbTe:Tl [6] and PbS:Tl [7] samples. The limiting concentrations of holes obtained by using thallium doping were 9×10^{19} cm^{-3} in PbTe and 5×10^{19} cm^{-3} in PbS, which corresponded to the resonance state energies of 0.2 eV in PbTe and 0.15 eV in PbS at 77 K. Thus the impurity electron levels in PbTe lie somewhat lower than the second maximum of the valence band (i.e., they slightly deepen into the second valence band), whereas in PbS these levels are between the principal and supplementary extrema in the valence band.

The shift of the band of Tl resonance states with temperature proved to be roughly identical in all three lead chalcogenides. The smallness of this shift implies that the Tl impurity states, as opposed to the In ones, do not leave the valence band over all the accessible temperature range. Therefore, no hopping conductivity, similar to that observed in PbTe [17] and $Pb_{1-x}Sn_xTe$ [18, 19] upon doping with indium under the conditions when the impurity states shift from the conduction to the forbidden band or reside at the very edge of the conduction band should be expected here.

The energy ε_{i} in the Tl-doped lead chalcogenides decreases with increasing temperature along with the energy separation between the two maxima of the valence band; as a result, the impurity states essentially do not move away from the edge of the second valence band. In any event, the thallium resonance

states are observed against the continuous background of the band spectrum corresponding to a relatively high density of states in the valence band. Because of this, a pronounced hybridization of the impurity and band states should be expected along with a marked broadening of the impurity band. The hybridization-aided width of the impurity band will be discussed below in the context of the resonance scattering of holes by Tl atoms (see Section 3.1). At this point, it is worth discussing two other reasons for broadening, namely, an overlap of the impurity wave functions and a spread of the Tl quasi-local energy levels due to composition inhomogeneity of the solid solution.

Analysis of the transport phenomena in the PbSe:Tl and PbS:Tl samples did not reveal a particular dependence of the impurity band position on the Tl concentration up to its highest values (the solubility limit). From this, a conclusion can be drawn regarding the weak overlap of the impurity wave functions and the smallness of the localization radius being not in excess of 10 A by an order of magnitude. This estimate from above bears evidence of strong localization of the impurity wave function. Hence it also follows that the wave-function overlap may not result in a perceptible broadening of the impurity levels, i.e., in washing out of the quasi-local states into an impurity band. The dependence of the impurity level position on the thallium content in the PbTe:Tl samples was observed at thallium concentrations $N_{Tl} \geqslant 0.3$ at.% [32], attesting that the overlap of the wave functions was somewhat stronger.

The thallium impurity states were studied by various techniques, among them the measurements and analysis of transport processes, in different IV–VI solid solutions based on lead chalcogenides, e.g., $PbSe_{1-x}S_x$ ($x = 0.5$) [33], $PbTe_{1-x}Se_x$ ($0 \leqslant x \leqslant 1$) [34], and $Pb_{1-x}Sn_xTe$ ($0 \leqslant x \leqslant 0.2$) [35].

A pronounced distinction between the positions of the Tl impurity band in PbSe and PbS (around 0.1 eV) suggests that ε_i depends essentially on the composition of the $PbSe_{1-x}S_x$ solid solution. This also means that one may expect a marked broadening of the impurity band due to the disorder in the Se and S atomic distributions over the sites of the chalcogen sublattice. The effect of broadening should be maximum in a solid solution with $x = 0.5$. In this connection, the electrophysical properties of $PbSe_{0.5}S_{0.5}$ with 1.2 at.% of Tl were investigated at various contents of sodium (acceptor) and excess lead (donor) permitting a change in the hole concentration on both sides with respect to the concentration in the sample doped with thallium only.

The dependences of the Hall and Seebeck coefficients on the temperature and hole concentration were qualitatively similar to those observed in the binary compounds. But the concentration-dependent Hall coefficient with a broad maximum at $p \approx 4 \times 10^{19}$ cm^{-3} testified to the existence of a wide thallium impurity band. Estimation of the position ε_i and the band width Γ at room temperature yields the following magnitudes: $\varepsilon_i \approx 0.18 \pm 0.03$ eV and $\Gamma \approx 0.1$ eV. The former is close to the midpoint between the corresponding values for PbSe and PbS, resulting in an approximately linear variation of $\varepsilon_i(x)$ at a rate $\partial\varepsilon_i/\partial x \approx -0.12$ eV. The sizeable broadening Γ supported by optical measurements (see Section 4.1) is related to various possible positions of Se and S atoms in the nearest coordination shell around a Tl atom that replaces Pb in a crystal lattice.

Experimental data on the Hall effect in the $PbTe_{1-x}Se_x$:Tl solid solution and their analysis demonstrated that with increasing x, the Tl impurity band shifts in an approximately linear fashion deeper into the valence band to its position in PbSe. The temperature coefficient of ε_i is $d\varepsilon_i/dT \approx -2 \times 10^{-4}$ eV K^{-1}, i.e., the temperature dependence of ε_i in the $PbTe_{1-x}Se_x$ solid solutions is roughly the same as in the pure PbTe and PbSe chalcogenides.

As regards the $Pb_{1-x}Sn_xTe$:Tl solid solution with 2 at.% Tl, a substitution of tin for lead shifts the Tl impurity band deeper into the valence band so quickly with increasing x that already at $x \geqslant 0.1$, the Tl band moves into the second valence band and ceases to affect transport processes. Practically all the holes are delocalized and the band concentration of holes is close to N_{Tl}. Against the background of high-density band states, the impurity band is notably spread on account of both the hybridization of impurity states with band states and the composition fluctuations in the solid solution.

The effect of pressure P on the energy position of resonance states in Tl-doped PbTe was studied synchronously with the pressure dependences of the superconductivity parameters (see Section 5) [36]. With increasing pressure, the Hall coefficient decreased, which was indicative of the increase of the hole concentration in the valence band through a partial transition of holes from quasi-local impurity states to delocalized band states. This means that the Tl impurity band goes deep into the valence band with increasing pressure. The assumption that the pressure dependence of the Hall coefficient mainly reflects changes in the concentration of light holes results in the following estimate: $\partial\varepsilon_i/\partial P \approx 1-2$ meV kbar^{-1}. The sign and the small value of the pressure coefficient of ε_i are consistent with evidence from the temperature-aided shift of the resonance-state band, i.e., a certain part (on the order of a quarter) of the temperature dependence of ε_i is dictated by thermal expansion of the crystal. Taking into consideration that the energy separation between nonequivalent extrema of the valence band increases at an essentially greater rate, the conclusion should be made that at high pressures the second valence band ceases to affect phenomena associated with the Tl resonance states.

2.3 Transport phenomena upon double doping

The above-reported results of transport phenomena studies in lead chalcogenides and their Tl-doped solid solutions made it possible to determine the energy position of the resonance-state band and its dependence on temperature, pressure and solid solution composition. At the same time it should be emphasized that the inference drawn above concerning the existence of the Tl resonance-state band in the lead chalcogenide valence band was mainly based on a quantitative comparison of data for samples with and without thallium. Thus it cannot be considered as well reliable without the evidence gathered by other methods described below. The more justified proof incident to the presence of the Tl resonance states was succeeded in providing concurrent doping of lead chalcogenides with thallium and an additional electrically active dopant that yields no impurity states.

It was double doping which revealed that the Fermi level locking owes its presence to the thallium impurity. According to the above-described model of resonance states and the thallium content corresponding to the $\rho(N_{Tl})$ saturation, the thallium acceptor action is restricted at low temperatures by the concentration at which the Fermi level reaches the impurity band.

When doping a sample with a supplementary acceptor impurity not producing impurity levels near the chemical potential and not changing the density of existing resonance states, the holes pass from acceptors to thallium atoms and the filling of the impurity band with holes is enhanced. Correct to the order of magnitude of the resonance band width, the Fermi level does not change upon supplementary doping and thus the hole concentration in the valence band remains constant. On donor alloying, the impurity band becomes depleted of holes and pinning of chemical potential also occurs. As long as the impurity band is partly filled, the pinning of the Fermi level takes place.

As a supplementary acceptor dopant in lead chalcogenides, Na [32, 37–40] and Li [41] along with excess chalcogen [38, 42] giving rise to acceptor-like intrinsic defects (metal vacancies) were commonly used. Excess lead played the part of additional donors [40, 43].

Figure 3 presents the composition dependences of the Hall concentration p of holes in PbTe:Tl with an additional Na impurity or excess Pb obtained for samples with a fixed Tl impurity content (the data are exemplified for $N_{Tl} = 0.5$ and 2 at.% at $T = 77$ K). The number density of sodium N_{Na} was plotted on the abscissa to the right, while that of the excess lead (N_{Pb}) to the left, and the absence of additional impurities and defects was matched by the zero point. With reference to Fig. 3, it can be seen that the composition dependences of the hole concentration exhibit broad ranges of the supplementary-impurity concentrations where p varies by an order of magnitude more weakly than N_{Na} and N_{Pb} do. There is every reason to believe that the hole concentration is stabilized over a broad range of additional impurities.

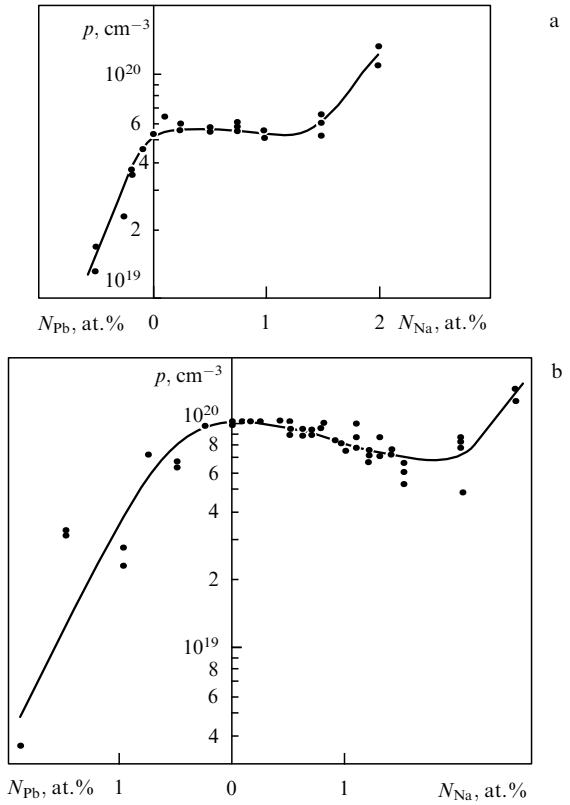

Figure 3. Plot of the hole concentration versus the amount of additional impurity introduced into PbTe:Tl: (a) $N_{Tl} = 0.5$ at.%; (b) $N_{Tl} = 2.0$ at.% [39].

A comparison between the data obtained for a series of samples with different thallium contents shows that the length of the interval over which p is stabilized increases approximately proportionally to the amount of thallium. The influence of Na on the hole concentration is small as long as the Na content in the sample is less than the thallium one. A greater content of additional impurities produces pronounced changes in the hole concentration in the valence band.

For large fixed contents of the sodium impurity (1–2 at.%), the introduction of thallium results in a reduction of the hole concentration, but no less than the stabilized level. To put it differently, at rather high acceptor concentrations thallium takes the role of a compensating donor. In this way, thallium in association with other electrically active impurities exhibits an amphoteric (donor-acceptor) property and can stabilize the hole concentration and, as a consequence, pinning of the chemical potential can occur.

Such behavior of the thallium impurity is explicable in the model of quasi-local states expounded earlier. Pinning of the Fermi level takes place by virtue of the high density of states in the valence band as long as it is localized within the band. The chemical potential leaves the band at a fixed Tl content and large additions of the supplementary impurity, resulting in a significant change in the hole concentration in the valence band.

Data for the length of the stabilization interval ΔN_i allow the evaluation of the number of states in the thallium band. For instance, for the series of samples with $N_{Tl} = 2$ at.% ($\approx 3 \times 10^{20}$ cm^{-3}) it was found that $\Delta N_i \approx 5.8 \times 10^{20}$ cm^{-3}, i.e., $\Delta N_i \approx 2N_{Tl}$; the same result is obtained for runs with $N_{Tl} = 0.5$ and 1 at.%. By this means there are two states per each impurity atom in the Tl impurity band, as in the In resonance-state band.

The presence of two states per Tl impurity atom provides an explanation for the amphoteric character of the given impurity. The Tl impurity substitutes bivalent lead in PbTe and, like Pb, it loses two electrons to form chemical bond with tellurium atoms. When the thallium atom is neutral, its third valence electron is localized in the band of the Tl impurity states. If all the Tl atoms were neutral, the impurity band would be half-filled with electrons, since the impurity band lies below the top of the valence band, and empty resonance states are populated by electrons from higher lying states. In so doing, the Tl atoms act as acceptors and go negative. In the absence of supplementary impurities, the quasi-local states are more than half-filled with electrons and the filling factor of the band with holes is $k_h < 0.5$. But if holes are further introduced, for instance, through doping with sodium, then they will pass to the Tl atoms. In doing so, thallium will behave as a donor and go positive, while the filling factor k_h therewith will increase. Supplementary doping with donors yields the reverse result.

In the case when each additional donor or acceptor impurity atom yields a single charge carrier (an electron or hole, respectively) per atom, the degree of filling of the Tl impurity band with holes can be represented as follows:

$$k_h = 0.5 + \frac{N_A - N_D - p}{2N_{Tl}}, \qquad (1)$$

where N_D and N_A are the concentrations of supplementary donors and acceptors, respectively. Estimation of k_h using formula (1) shows that without additional doping, the

maximum degree of band filling is in the vicinity of 1/3 (for $N_{Tl} = 2$ at.%). Supplementary doping with sodium allows k_h enhancement up to the point corresponding to the complete filling of the impurity band ($k_h \approx 1$), whereas introduction of donors can result in a total release of holes from the Tl band ($k_h = 0$) and an upward displacement of the chemical potential beyond the impurity band edge.

A single level of chemical potential pinning observed in experiments with two impurity states per Tl atom suggests the electron correlation energy U in the impurity state to be rather small (less than the impurity band width) or even negative.

Saturation of the Hall concentration upon the variation of the supplementary impurity content and a considerable length of the stabilization interval allow more precise determination of the quasi-local level position Γ and its temperature and impurity concentration dependences than in the case of simple thallium doping. At $T = 77$ K and relatively low thallium content (0.3 at.%) in PbTe, it was found that the energy depth of impurity levels in the valence band was $\varepsilon_i = 0.16$ eV [32, 38]. With a rise in Tl concentration to 1–2 at.%, ε_i increases to ≈ 0.2 eV in compliance with the degree of hole concentration saturation upon simple doping. Figure 3 also displays that stabilization of the concentration turns out to be incomplete and the Hall concentration of holes slowly decreases with increasing Na content, being brought about by the displacement of the Tl impurity band toward the valence band edge on addition of Na. The $\varepsilon_i(N_{Na})$ dependence has a nearly linear shape with $\partial\varepsilon_i/\partial N_{Na} \approx -(40-50)$ meV/at.% [32]. The rate of impurity level displacement with temperature may be characterized by the derivative $\partial\varepsilon_i/\partial T \approx -(2-3)\times 10^{-4}$ eV K^{-1} [32], i.e., the impurity band approaches the valence band edge somewhat slower than the second extremum of the valence band.

We now consider the temperature dependence of the Hall coefficient R upon double doping. As noted above, changing sodium to thallium for an acceptor impurity in PbTe markedly increases the growth rate of the Hall coefficient with temperature (over the range of relatively low temperatures) through thermal activation of holes from the valence band to the Tl impurity band. Additional sodium doping of lead telluride with thallium makes an even greater impact on the temperature behavior of R. As seen from Fig. 4, the initial growth of R with temperature is weakened upon supplementary sodium doping and then gives way to a descending curve for sufficiently large amounts of Na. The maximum in the temperature dependence of R disappears in the process. The change of sign of the derivative dR/dT was never observed in p-type PbTe samples without thallium, but this result can be explained within the model of resonance states.

Let us take a look at the dependence of the derivative dR/dT on the filling factor k_h of filling the Tl impurity band with holes, which can be related to the difference between the chemical potential and the midpoint of the band, $\mu - \varepsilon_i$. In particular, if the density of impurity states $g_i(\varepsilon)$ is symmetric about ε_i and $\mu = \varepsilon_i$, then the band is half-filled and $k_h = 0.5$ for any temperature. Assuming that the impurity-state holes do not contribute to conductivity, the authors of Ref. [38] derived the following expression for dR/dT, proportional to the derivative dp/dT of the hole concentration in the valence band:

$$\frac{dR}{dT} \sim -\frac{dp}{dT} = \frac{dp_i}{dT} = \frac{g_0 S_0}{1+S_0}\left(k_B \frac{S_1}{S_0} - \frac{d\varepsilon_i}{dT}\right), \qquad (2)$$

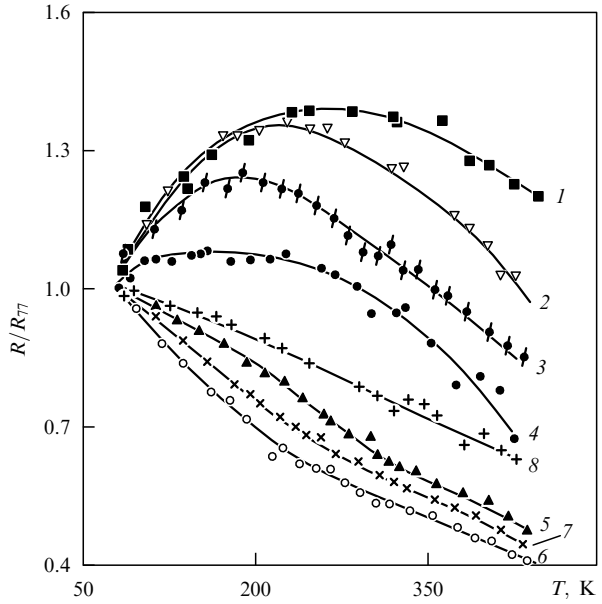

Figure 4. Temperature dependence of the Hall coefficient evaluated in the relative units (R/R_{77}) for various compositions of the $Pb_{0.98-x}Tl_{0.02}Na_xTe$ samples [39] (R_{77} is the Hall coefficient at 77 K, x is measured in at.%): (*1*) 0; (*2*) 0.15; (*3*) 0.4; (*4*) 0.5; (*5*) 1.0; (*6*) 1.5; (*7*) 2.0; and (*8*) 2.5.

where p_i is the hole concentration in the impurity band, g_0 is the density of states in the valence band close to the impurity band, k_B is the Boltzmann constant, and S_n ($n = 0, 1$) are the integrals defined as

$$S_n = \frac{1}{g_0}\int_{-\infty}^{\infty}\left(-\frac{\partial f}{\partial\varepsilon}\right) g_i(\varepsilon)\left(\frac{\varepsilon-\mu}{k_B T}\right)^n d\varepsilon. \qquad (3)$$

Since g_i is an even function of $\varepsilon - \varepsilon_i$ and $(-\partial f/\partial\varepsilon)$ is an even function of $\varepsilon - \mu$, the integral S_1 goes to zero for $\mu = \varepsilon_i$ (i.e., at $k_h = 0.5$) because in this case an odd function of $\varepsilon - \mu$ is under the integral. Both the integrals S_0 and S_1 are positive for $\mu < \varepsilon_i$ ($k_h < 0.5$) and consequently the first term in formula (2) is also positive. For $\mu > \varepsilon_i$ ($k_h > 0.5$), we have $S_0 > 0$, $S_1 < 0$ and the first term in (2) is negative.

Such a dependence of S_1 on k_h is representative of the fact that for relatively low band filling with holes and as the temperature increases, the thermal activation of holes from the valence band to the impurity band increases, the hole concentration in the valence band decreases, and the Hall coefficient grows, whereas at high degrees of band filling with holes, the thermal activation of holes from the impurity band into the depth of the valence band prevails and the Hall coefficient decreases. If we approximate the $g_i(\varepsilon)$ function with the Lorentzian of width Γ [see below Eqn (5)], then it develops that the first term in formula (2) is a maximum in absolute magnitude for $\varepsilon - \mu \approx \pm\Gamma/2$, which at $k_B T \ll \Gamma$ yields values for the hole filling factor k_h equal to 1/4 and 3/4.

The experimental dependence of the derivative dR/dT on the filling factor k_h agrees satisfactorily with the calculated results (see Fig. 5). This agreement means that the temperature dependence of the position of the center of the band ε_i exerts a minimal effect on R, whence it follows that $|d\varepsilon_i/dT|$ is no more than 10^{-4} eV K^{-1} on the order of magnitude, in line with the above-made estimates.

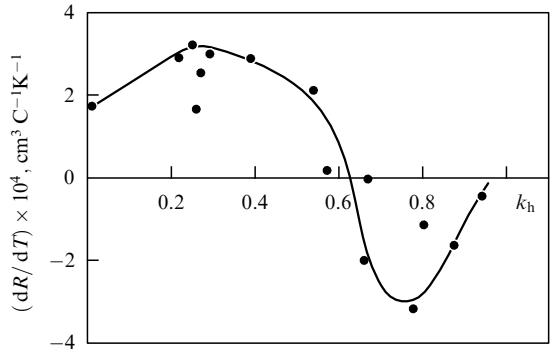

Figure 5. Rate of change of the Hall coefficient with temperature (dR/dT) at 100 K against the degree of filling of the thallium quasi-local states with holes in the PbTe:(Tl, Na) samples [39]; $N_{Tl} = 2$ at.%.

When studying temperature dependence of electrical conductivity σ, some additional conductivity [39] increasing with temperature within the interval 100 – 300 K was detected in several PbTe samples with double doping. To account for this conductivity, it was suggested that the impurity band consists of two narrow subbands of propagating states separated by the mobility gap. Thermal activation of carriers from the filled into the empty subband through the mobility gap produces conduction over impurity-band states, which shows an increase with rising temperature. This hypothesis, however, failed to be confirmed and did not receive further development.

Completing the presentation of the results obtained for lead chalcogenide samples with double doping, it is worth citing the works wherein thallium was employed with the aim of investigating the properties of other impurities, for instance, as a supplementary impurity in studies of hopping conductivity over In impurity atoms in $Pb_{0.8}Sn_{0.2}Te$ [44] and Sn impurity states in $PbTe_{1-x}S_x$ through simultaneous measurements of kinetic coefficients and the Mössbauer effect [45, 46].

3. Hole scattering by thallium impurity atoms

Research into the transport phenomena in thallium-doped lead chalcogenides has culminated in the discovery of clearly defined resonance scattering of holes by Tl impurity atoms. The resonance scattering of charge carriers was previously discussed for several III – V [47] and II – VI [48] compound semiconductors, but the most detailed and diversified information about this process has only been gathered for lead chalcogenides doped with thallium. The results of these studies provide the subject matter for the present section.

3.1 Hole mobility and thermo-emf in thallium-doped lead chalcogenides

The most direct and reliable evidence of the resonance character of hole scattering from thallium impurity atoms was originally produced in measuring the dependences of electrical conductivity and the Hall coefficient on the Tl impurity concentration in single-crystal PbTe [49]. Figure 6 displays experimental curves of the Hall mobility of holes in lead telluride alloyed with two different acceptor dopants (thallium or sodium) as functions of the hole concentration increasing with the dopant content. At low temperatures, 4.2

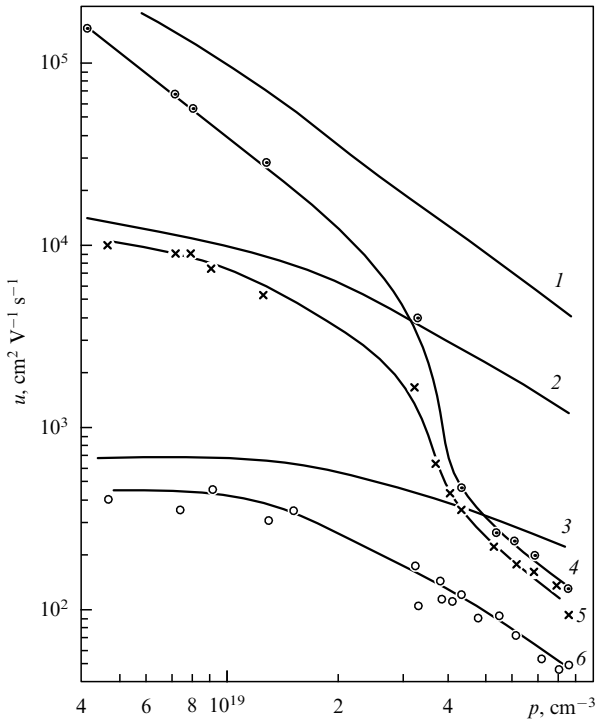

Figure 6. Concentration dependence of the Hall hole mobility u in the p-PbTe:Tl crystals [49]: (*1*) – (*3*) experimental results for PbTe:Na; (*4*) – (*6*) for PbTe:Tl; T, K: (*1*), (*4*) 4.2; (*2*), (*5*) 77; and (*3*), (*6*) 300.

and 77 K, the dominating mechanism of scattering in lead chalcogenides is determined by hole scattering from impurities.

With reference to Fig. 6, it can be seen that the mobilities in the thallium- and sodium-doped samples differ only slightly at relatively low Hall hole concentrations approaching $\sim 5 \times 10^{19}$ cm^{-3}. Estimates of the cross sections relevant to the hole scattering by impurities yield magnitudes of the order of 10^{-16} cm^2, i.e., ordinary cross sections for charge carrier scattering from different impurities in lead chalcogenides. Considering the smallness of this cross section and the inefficiency of Coulomb scattering from charged impurity atoms, it should be inferred that the holes in the range of energies far from the impurity band are scattered mainly from the highly localized impurity potential core. The cross section itself is independent of the energy for such *s* scattering and the mobility shows a fall with rising chemical potential due to the growth of the carrier velocity.

As the hole concentration increases beyond 5×10^{19} cm^{-3}, a sharp decrease in the mobility is found in PbTe:Tl when the chemical potential reaches the impurity band (and the thallium concentration comprises 1 – 2 at.%). The mobility drop and rise in the corresponding cross section for hole scattering proved to be particularly high at low temperatures: by a factor of 8 – 10 for 77 K and 30 – 50 for 4.2 K. The effect observed was explained by the authors of Ref. [49] using the mechanism of hole resonance scattering from Tl quasi-local states.

Another series of experimental results was gathered simultaneously, which bore evidence of strong resonance scattering in PbTe:Tl. Measurements on the Nernst – Ettingshausen effect in Refs [40, 49], which refers to current-free effects, ruled out the possibility that the observed mobility

drop resulted from the influence of extended defects like grain boundaries and microcracks — the Nernst mobility in PbTe:Tl, just as the Hall mobility, turned out to be significantly lower than in PbTe:Na.

The intensity of resonance scattering depends essentially on the resonance band width. Hybridization of the impurity and band states could give rise to both resonance scattering and broadening of the impurity band. Further causes of broadening are an overlap of the impurity wave functions and a spread of the impurity energy levels on account of the sample's inhomogeneity and disorder in the impurity distribution.

If the hybridization of impurity states occurs with the participation of more than one band (for instance, with bands of light and heavy holes), then the total width Γ of the band can be represented as the sum of partial broadenings γ_i stemming from hybridization with each of the bands and certain variables describing broadening due to other mechanisms. Using the Breit – Wigner formula for the resonance s scattering yields the time relaxation in the form [38]

$$\tau_{res}(\varepsilon) = \frac{\hbar g_0}{\gamma g_i(\varepsilon)}, \tag{4}$$

where γ is the broadening of the resonance energy level through hybridization of impurity states with states of the band in which the carrier scattering is considered (for example, in the light-hole band), g_0 is the density of states in the allowed band close to the impurity band, and $g_i(\varepsilon)$ is the density of impurity states depending on the total width of the band Γ, the latter being conditioned by all the mechanisms of broadening. If it is the hybridization that is mainly responsible for the broadening, then the density of impurity states $g_i(\varepsilon)$ is given by the Lorentzian

$$g_i(\varepsilon) = \frac{N_{Tl}}{\pi} \frac{\Gamma}{(\varepsilon - \varepsilon_i)^2 + (\Gamma/2)^2}. \tag{5}$$

When deducing this formula, it was considered that in the impurity band there are two states per thallium atom, i.e., the total number of states in the band comes out as $2N_{Tl}$.

Formulas (4) and (5) were used as the basis in deriving the following expression for the electrical conductivity of strongly degenerate holes in one of the subbands on the condition that resonance scattering dominates and with the constraint $k_B T \ll \Gamma$ [38]:

$$\sigma = \frac{(3\pi^2)^{1/3} e^2 p^{4/3}}{4\pi\hbar N_{Tl}} \frac{m_d^*}{m_c^*} \frac{\Gamma}{\gamma} \left\{ 1 + \tan^2 \left[\pi \left(k_h - \frac{1}{2} \right) \right] \right\}, \tag{6}$$

where m_d^* and m_c^* are the effective masses for the density of states and conductivity, respectively.

With the contributions of light and heavy holes to electrical conductivity, formula (6) defines the partial conductivity for one of the bands, whereas the experimentally established total electrical conductivity depends on the ratio b between the mobilities of light and heavy holes, which usually remains a mystery. At first glance, it would seem that the determination of two unknown parameters γ/Γ and b from one experimental quantity σ is almost impossible. Under resonance scattering conditions the parameter b is equal to the ratio of the partial broadening for the subband of light holes to that of heavy holes, γ_L/γ_H, so that the γ_L/Γ and γ_H/Γ ratios may be chosen for the adjustable parameters. In this case, the inequality $\gamma = \gamma_L + \gamma_H \leqslant \Gamma$ must hold. In the course of the calculation, it has been ascertained [38] that the above inequality does not hold for magnitudes of b noticeably different from unity, while at $b \approx 1$, one obtains the values $\gamma/\Gamma \cong 1$ and $\gamma_H/\gamma_L \cong 2$. Thus, the mobilities of light and heavy holes differ little in circumstances where resonance scattering is dominant and the broadening of thallium impurity band is mainly accounted for by the hybridization of impurity states with the states in the valence band; in so doing, the hybridization with the second valence band makes twice as much contribution to the band broadening than that with states close to the primary extremum.

The separation of light and heavy hole contributions to electrical conductivity also permitted the cross sections of resonance scattering for the holes of the two types to be determined. These cross sections turned out to be of order 10^{-14} cm^2, i.e., two orders of magnitude greater than the cross section for potential scattering.

The occurrence of clearly defined resonance scattering testifies that if the Tl atoms are centers with negative correlation energy, then the $|U|$ magnitude is relatively small and does not exceed the width Γ of the impurity band.

Similar results for the hole-concentration-dependent Hall and Nernst mobilities were also obtained for the PbSe samples [29]: under Tl doping, the mobility reduced and for the hole density $p \sim 10^{20}$ cm^{-3} and $T = 85$ K it proved to be 5 – 6 times less than in the Na-doped samples.

Resonance scattering can also have a pronounced effect on the dependence of the Seebeck coefficient α on the hole concentration, bringing about the appearance of a deep minimum in the relevant curve [28]. As is well known, the thermoelectric power varies directly as the scattering parameter r, which in the case of strong degeneracy is given by the following expression:

$$r = \left(\frac{\partial \ln \tau}{\partial \ln \varepsilon} \right)_{\varepsilon = \mu}. \tag{7}$$

In particular, for standard dispersion in strongly degenerate samples one obtains

$$\alpha = \frac{\pi^2}{3} \frac{k_B}{e} \frac{k_B T}{\mu} \left(r + \frac{3}{2} \right). \tag{8}$$

From formulas (4), (5) and (7), it follows that in circumstances where resonance scattering is dominant, we have

$$r = \frac{2\mu(\mu - \varepsilon_i)}{(\mu - \varepsilon_i)^2 + (\Gamma/2)^2}. \tag{9}$$

This quantity reverses sign at $\mu = \varepsilon_i$, while at $\mu - \varepsilon_i = -\Gamma/2$, it passes through a minimum equal to $-2\mu/\Gamma$, thus resulting in the appearance of a deep minimum in the thermo-emf curve and even in a change of sign of the thermoelectromotive force [28]. Theoretical evaluation of the thermo-emf permitted the $\alpha(p)$ curve to be constructed, which shows the best correlation with experimental data at the following values of parameters: $\varepsilon_i = 0.21$ eV and $\Gamma = 0.04$ eV in the example of PbTe:Tl. Analogous results for the thermoelectromotive force were also obtained in other Tl-doped lead chalcogenides and solid solutions: PbSe [29], PbS [7], $PbSe_{1-x}S_x$ [33], and $Pb_{1-x}Sn_xTe$ [50].

3.2 Resonance scattering in the case of double doping

New information about the resonance scattering of holes was gathered in experiments on additional alloying of the PbTe:Tl samples with dopants that produce no impurity states, namely, Na [37, 38] and Li [37] acceptors as well as hyperstoichiometric lead, which has a donor effect on them [43]. Doping with supplementary acceptors (not changing the density of the Tl impurity states) increases the degree of impurity band filling with holes in compliance with Eqn (1). In doing so, the Fermi level moves over the impurity band and may fall into regions with different densities of impurity states. By reference to formula (5) for the impurity state density and assuming $k_B T \ll \Gamma$, a relationship can readily be obtained between the factor of band filling with holes and the position of chemical potential with respect to the impurity band center:

$$\mu - \varepsilon_i = \frac{\Gamma}{2} \tan\left[\pi\left(k_h - \frac{1}{2}\right)\right]. \qquad (10)$$

From expressions (4), (5) and (10), one can find the filling factor dependence of the conductivity of degenerate samples over the region of resonance scattering, which is described by formula (6).

Because, as indicated above, we have $k_h \approx 0.3$ in the absence of supplementary doping in PbTe:Tl and the density of impurity states is maximum at $k_h = 0.5$, the additional doping with acceptors initially lowers the electrical conductivity and then afresh tends to step up σ on further increasing the acceptor content.

The experimental curve in Fig. 7 is well suited to this prediction. As may be seen from the figure, the resistivity ρ depends on the filling factor k_h in the same fashion as the density of impurity states g_i depends on the Fermi level, which was determined from existing data on superconductivity (see below, Section 5) and low-temperature heat capacity (Section 4.2).

The peak in the $\rho(N_{Na})$ curve resulted from resonance scattering constitutes one of the most striking illustrations of the presence of a thallium resonance state within the valence band.

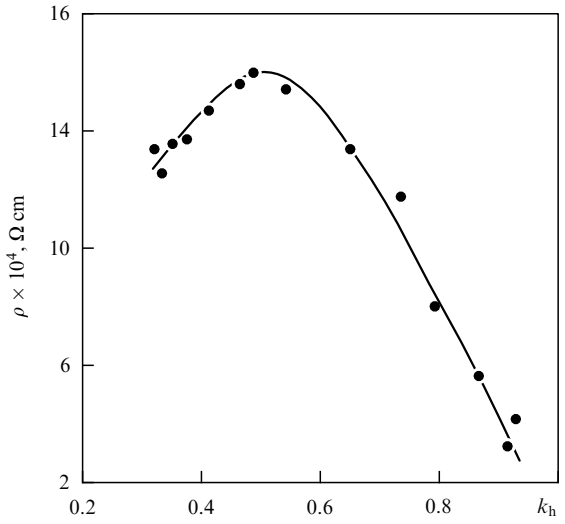

Figure 7. Plot of the resistivity ρ of $Pb_{0.98-x}Tl_{0.02}Na_xTe$ samples versus the degree of filling of the thallium resonance states with holes k_h at 4.2 K [37]. The sample with $k_h \approx 0.3$ is a single crystal, and the rest are ceramic polycrystals.

Reference to formula (6) shows that, as the factor of band filling with holes k_h increases to 0.5 by additional doping, the calculated electrical conductivity of a sample decreases by a factor of approximately 1.5 in comparison with the case of no additional acceptors. This result also fits well with experimental data depicted in Fig. 7.

In the strict sense, the smallness of $(lk_F)^{-1}$, where l is the mean free path and k_F is the wave vector of holes at the Fermi level, provides the criterion of applicability for the formulas employed above. Evaluation of this quantity in the region of resonance scattering showed that in real situations $lk_F \sim 1$ and thus the calculated results given above for kinetic coefficients should be considered as appraised [38]. However, a reasonable agreement between the calculated and experimental findings testifies that hybridization of the band and impurity states is not strong to the extent that it may result in a drastic rearrangement of the electronic spectrum and, in particular, in the appearance of a gap in the density of states near the middle of the impurity band .

The dependence of the thermoelectromotive force on the concentration of supplementary acceptors is governed by the fact that the thermoelectric power is linear in the scattering parameter r. The latter, in compliance with Eqn (9), has a maximum and minimum for $\mu - \varepsilon_i = \pm\Gamma/2$ to check with the magnitudes of k_h equal to 0.75 and 0.25, respectively. The experimental $\alpha(k_h)$ dependence in a series of PbTe samples with $N_{Tl} = 2$ at.% goes through a maximum and minimum in the vicinity of these values, as indicated by Fig. 8 [51].

Leaning upon facts that at sufficiently low temperatures ($T \leqslant 100$ K) the resonance scattering in the PbTe samples doped with 1–2 at.% Tl presents a dominant mechanism of scattering, the authors of Ref. [51] obtained a solution of the inverse problem by finding the function of the density of states from the experimental k_h-dependence of the thermoelectromotive force. From formulas (4) and (7), it follows that

$$r = -\left.\frac{\partial \ln g_i}{\partial \ln \varepsilon}\right|_{\varepsilon=\mu}. \qquad (11)$$

This quantity as a function of k_h was determined from experimental values of the thermoelectric power α. Integ-

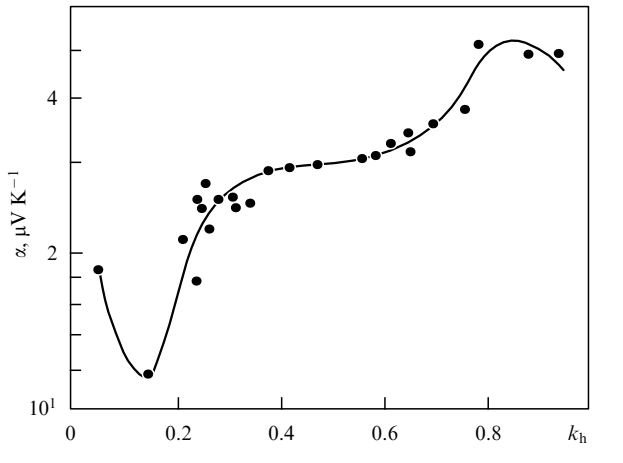

Figure 8. Variation of the thermoelectric power α for a PbTe sample alloyed with 2 at.% Tl and an additional dopant, as a function of the degree of filling k_h of the Tl impurity band with holes at 120 K [51].

rating (11) with respect to the wave number yields [51]

$$g_i(k_h) = -2N_i \int_0^{k_h} \frac{r(k)}{\mu(k)}\, dk\,. \qquad (12)$$

The last formula takes into consideration that the total number of states in the impurity band equals $2N_i$. The function $\mu(k_h)$ is determined from the Hall concentration measurements using the parameters of the band of light holes. In so doing, the position of the chemical potential μ with respect to the impurity band midpoint is found insufficiently accurate and we have to iterate numerically an integral for the quantity $\mu - \varepsilon_i$ to be calculated:

$$\Delta\mu \equiv \mu - \varepsilon_i = 2N_i \int_{0.5}^{k_h} \frac{dk}{g_i(k)}\,. \qquad (13)$$

Given g_i and $\mu - \varepsilon_i$ as functions of k_h, we arrive at the dependence of the density of states g_i at the Fermi level on the chemical potential μ, i.e., the entire curve $g_i(\varepsilon)$.

To realize the computation scheme outlined above, the influence of heavy holes on the thermoelectromotive force has to be taken into account. The bell-like curve $g_i(\varepsilon)$ was constructed with allowance for the growth of the energy gap between valence subbands with increasing Na content. Such growth was found from independent measurements [52] and thus it is corroborated by the results of thermo-emf analysis in the PbTe samples doubly doped with Tl and Na. Figure 9 presents $g_i(\Delta\mu)$ curves plotted for various values of the derivative $d\Delta\varepsilon_v/dN_{Na}$ in the range of 0.01 to 0.1 eV/at.%. At $\varepsilon < \varepsilon_i$, the shape of the curve is independent of the chosen magnitude of the derivative and is well described by a Lorentzian with a halfwidth $\Gamma/2 \sim 0.02-0.03$ eV. At $\varepsilon \approx \varepsilon_i$, the curve possesses a nearly flat peak, while at $\varepsilon > \varepsilon_i$, the density of states diminishes more slowly with increasing ε than it grows for $\varepsilon < \varepsilon_i$. This asymmetric shape of the density-of-resonance-states curve may be explained qualitatively by the enhancement of hybridization and the growth of the parameter Γ with increasing energy due to a rapid build up of the density of band states as we go deep into the second valence band.

The Nernst–Ettingshausen effect (NEE), which also depends to a large measure on the parameter r of hole scattering, was studied in some detail in PbTe samples doubly doped with Tl and Na [40]. For strong degeneracy, in circumstances where the standard law of hole dispersion is obeyed, the Nernst–Ettingshausen coefficient is expressed as

$$Q = \frac{\pi^2}{3}\,\frac{k_B}{e}\,\frac{k_B T}{\mu}\, rR\sigma\,. \qquad (14)$$

As is the case with sodium doping of lead chalcogenide, the experimentally found coefficient Q proves to be negative in doubly doped PbTe samples. The mobility-proportionate quantity $|Q(k_B/e)^{-1}|$ (the Nernst mobility) is significantly lower than in sodium-doped samples with the same concentration of holes. This lends support to the presence of a strong resonance scattering.

At the same time, an appraisal of the effective scattering parameter r_{eff} using formula (14) revealed that the magnitude of $|r_{eff}|$ is anomalously high [$r_{eff} \approx -(17-18)$] for the factors of resonance band filling with holes in the vicinity of 0.25 ($\mu - \varepsilon_i \approx -\Gamma/2$). As indicated by the foregoing [see formula (9)], for these values of k_h under conditions of strong resonance scattering, the parameter r has a negative sign and its modulus is much greater than unity. Thus, the negative values of r_{eff} obtained for $k_h < 0.5$ may be explained by fast enhancement of resonance scattering as the hole energy increases.

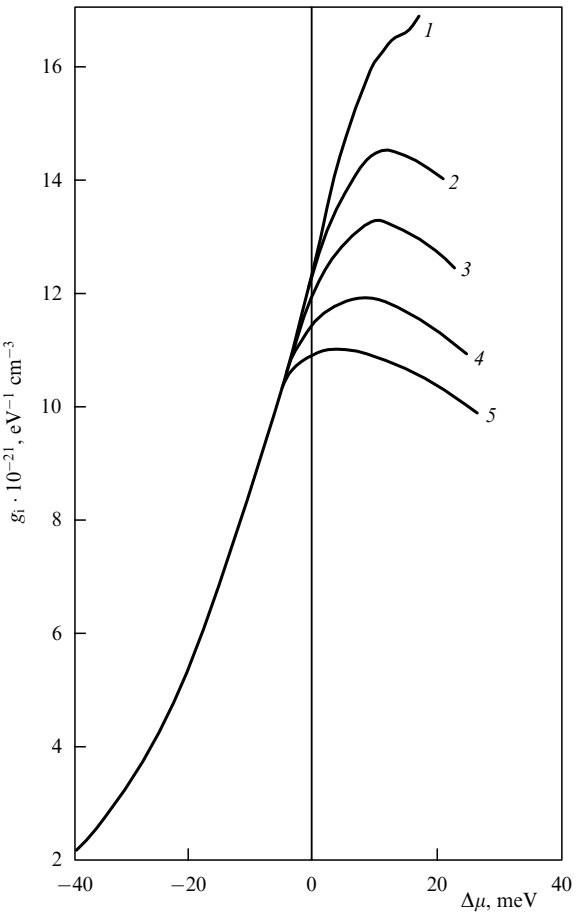

Figure 9. Energy dependence of the density of resonance states in PbTe:(Tl, Na) calculated in the framework of a two-band model from data for the thermo-emf in a series of samples with $N_{Tl} = 2$ at.% [51] at various $d\Delta\varepsilon_v/dN_{Na}$: (*1*) 10; (*2*) 20; (*3*) 30; (*4*) 50; and (*5*) 100 meV/at.%.

With a rise in k_h above 0.25 ($\mu - \varepsilon_i > -\Gamma/2$), the parameter r for resonance scattering shows an increase in conformity with expression (9), then it becomes positive for $k_h > 0.5$ and passes through a maximum at $k_h = 0.75$ ($\mu - \varepsilon_i = \Gamma/2$). Although the parameter r_{eff} determined from the experimental value of Q grows with k_h, it nowhere changes sign. Experimental dependences of the Nernst–Ettingshausen coefficient on the concentration of Na used as an additional impurity (see Fig. 10) are nonmonotonic and have a rather complex shape characterized by several maxima and minima. This trait of NEE is difficult to explain on resonance scattering grounds alone and for a qualitative interpretation of experimental curves it was taken into account that the NEE pattern observed can be essentially complicated because of the presence of spatial inhomogeneities in the distribution of impurities, for instance, thallium, which produces resonance states, and a number of additional impurities changing the degree of band filling with holes.

Under conditions of strong resonance scattering, the inhomogeneities are of rather specific importance. It is customary to scrutinize the inhomogeneities of the charge

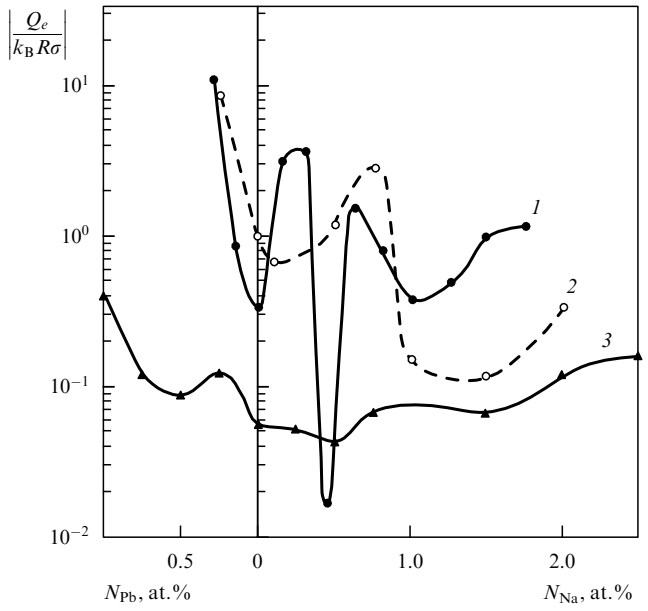

Figure 10. Plot of the dimensionless Nernst – Ettingshausen coefficient $|Qe/k_B R\sigma|$ at 120 K versus the amount of additional impurity introduced into PbTe:Tl [40]; N_{Tl}, at.%: (*1*) 0.3; (*2*) 0.5; and (*3*) 2.0 [40].

carrier concentration and consider the kinetic coefficients to be independent of the mobility fluctuations [53]. Pinning of the chemical potential through the mediation of the resonance levels causes a sample to become homogeneous in the carrier concentration despite substantial fluctuations in the impurity distribution. At the same time, the concentration inhomogeneity of thallium and a supplementary impurity affects the nonuniformity of the factor of impurity band filling with holes and, thus, the fluctuations of the scattering parameter r. This type of inhomogeneity was first examined in the context of the explanation of experimental data on transport phenomena in the thallium-doped lead chalcogenides [40]. It is responsible for nonuniformities in the thermoelectric power, which in turn initiate eddy currents in a sample. The eddy-current-induced Hall effect on makes a significant additional contribution to the effective coefficient Q, particularly in the case that the mean local value of the Nernst – Ettingshausen coefficient is small.

Estimation of the effective Nernst – Ettingshausen coefficient by the Herring method [53] permitted derivation of a formula containing a series of terms of different origin, which show various and nonmonotonic dependences on the hole filling factor k_h, much like the above-considered parameters τ_{res} and r. Although the particular calculation with the given formula would require simplifying assumptions and knowledge of a diversity of parameters, it seems likely that superposition of several terms with different signs could give an observed picture of the NEE dependence on the degree of filling of the impurity band. By this means, in circumstances where strong resonance scattering occurs, the nonuniformity of the scattering parameter r may account for observed NEE irregularities in the PbTe:(Tl, Na) samples.

Whilst the effective kinetic coefficients are not influenced by the microinhomogeneities of mobility, the large-scale mobility inhomogeneities, which are also possible in the presence of impurity concentration fluctuations under conditions of resonance scattering, reveal themselves in the kinetic coefficient dependences on the sample sizes. Thus, Boĭko et al. [54] observed the resistivity of PbTe:Tl whiskers to depend on their diameter. Kaĭdanov [55] reported on the resonance scattering of holes in the coarse-blocked (with low-angle grain boundaries) PbTe:(Tl, Na) films on mica.

Comparing numerous and detailed experimental data on the resonance scattering of holes from Tl atoms with the results of studying transport phenomena in indium-doped lead chalcogenides, one can recognize essential differences in the process of charge carrier resonance scattering by these two group III impurity atoms. At low (liquid-helium) temperatures, no resonance scattering was observed in the samples doped with indium and additional impurities. This finding fits well with the detection of long-term relaxation in PbTe:In [9, 10], which is explained by structural rearrangement of the impurity center and its surroundings upon changes in its charge state [11, 12], and the lack or small magnitude of the effect in PbTe:Tl (see below Section 4.3). The long-term relaxation in PbTe:In dies out for $T > 20$ K and an additional scattering manifests itself concurrently [56, 57]. The latter was interpreted in Ref. [57] as resonance scattering with the participation of phonons. Strong resonance scattering from thallium atoms at low temperatures demonstrates that no essential rearrangement occurs with changes in their charge states.

Effective attraction between the charge carriers localized on a single impurity center [14, 15] must also prevent resonance scattering. Hence, it follows that the In atoms in lead chalcogenides can act as centers with negative Hubbard energies, whereas the Tl atoms can not.

The In impurity levels in the $Pb_{1-x}Sn_xTe$ solid solutions are lowered with increasing x; they escape from the conduction band and find themselves in the valence band in the SnTe samples. Such processes are accompanied by clearly defined resonance scattering [58], which is a close match to that observed in PbTe:Tl. From this it is inferred that the various symmetry of electron wave functions significantly affects the hybridization of impurity and band states as well as resonance scattering in IV – VI compound semiconductors. If it is assumed [1, 2] that the indium impurity states are described by even s functions in reference to the metal sublattice site where the impurity group III atoms are positioned, then the parities of impurity states and electron wave functions of L_6^- symmetry are the reverse of each other in the proximity of the lead chalcogenide conduction-band edge. At a hole energy comparable to the energy gap ε_g, the impurity states deep in the valence band are described by the superposition of wave functions L_6^- and L_6^+, i.e., they involve a component whose parity coincides with that of the impurity s functions.

In what follows, we consider a particular correlation between the process of resonance scattering and superconductivity stemming from the presence of resonance states (Section 5) as well as analogous linkage of resonance scattering with the results of studying low-temperature heat capacity (Section 4.3).

3.3 Thermoelectric figure of merit in the case of resonance scattering

The above-given formulas (8) and (9) demonstrate that resonance scattering is favorable for the growth of the Seebeck coefficient (and, consequently, of the Peltier coefficient) on filling the impurity band more than by half with charge carriers. This circumstance offers possibilities of enhancing the thermoelectric figure of merit of semiconduc-

tors

$$Z = \frac{\alpha^2 \sigma}{\lambda}, \tag{15}$$

where λ is the total thermal conductivity. The formula written above defines the efficiency of thermoelectric current sources and the cooling factor of refrigerators.

Resonance scattering provides an example of selective scattering whereupon some groups of carriers may be scattered much more strongly than others. For the position of resonance states within the range of carrier energies below the chemical potential μ, the charge carriers with relatively low energies ($\varepsilon - \mu < 0$) are scattered far better than those with relatively high energies ($\varepsilon - \mu > 0$), resulting in an enhancement of the mean carrier energy of the flux and thereby in an increase of the Seebeck coefficient. If the mobility of carriers is not too far reduced in the process, the magnitude of the thermoelectric figure of merit (15) may be increased as well. Computations performed in Refs [8, 59, 60] lent support to these inferences and permitted the determination of the optimal parameters for resonance scattering, which yield the maximum gain in thermoelectric efficiency.

It follows from Eqns (4) and (5) that a strong energy dependence of the relaxation time $\tau_{res}(\varepsilon)$ for resonance scattering is given by the expression

$$\tau_{res} = \tau_{res}^{(0)} \left[1 + \left(\frac{\varepsilon - \varepsilon_i}{\Gamma/2} \right)^2 \right]. \tag{16}$$

Under strong degeneracy ($\mu^* \gg 1$) in circumstances where resonance scattering and conventional scattering from acoustic phonons (described by the relaxation time $\tau_0(\varepsilon)$) proceed simultaneously, the influence of resonance scattering on the thermoelectric variables may be characterized by three dimensionless parameters:

$$A = \frac{\tau_0(\mu)}{\tau_{res}^{(0)}}, \quad M = \frac{\mu - \varepsilon_i}{\Gamma/2}, \quad \Gamma^* = \frac{\Gamma}{k_B T}. \tag{17}$$

The first parameter A, which is proportional to the concentration of resonance centers, stands for the contribution of resonance scattering at an energy $\varepsilon = \varepsilon_i$. The second parameter M varies proportionally with the deviation of the chemical potential from the impurity band center. The magnitude of M is uniquely related to the factor of impurity band filing with holes [see Eqn (10)] and can be varied through additional doping.

It is common for the thermal conductivity λ of semiconducting thermoelectric materials to result predominantly from heat transfer by phonons and the maximum Z corresponds to the same optimal parameters of resonance scattering as those correlating with the maximum of the specific thermoelectric factor $\alpha^2\sigma$. Figure 11 displays the plots of the $\alpha^2\sigma$ factor versus parameter A characterizing the relative intensity of resonance scattering at different numerical values of the parameter M. The curves at hand were obtained by numerical calculations; they are consistent with what is expected for the case of moderately strong degeneracy ($\mu^* = 6$) and a fulfilment of the equality between the band halfwidth and the energy parameter $k_B T$, i.e., $\Gamma^*/2 = 1$. As may be inferred from the figure, the curves have flattened maxima. The highest value of the $\alpha^2\sigma$ factor, which is three times as great as the corresponding value in the absence of

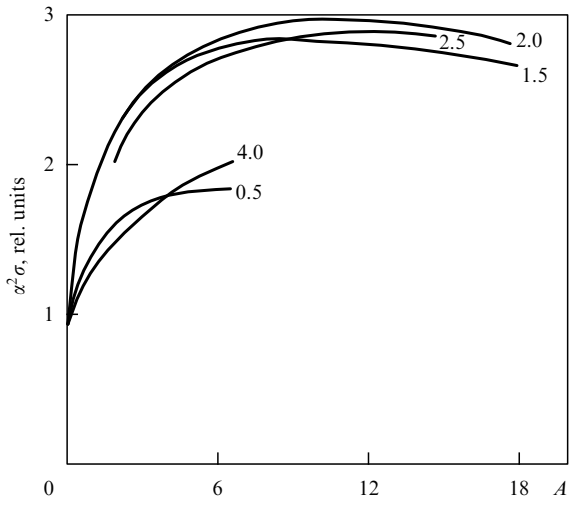

Figure 11. Variation of the specific thermoelectric power $\alpha^2\sigma$ with dimensionless parameter A characterizing the contribution of resonance scattering ($\Gamma^*/2 = 1$, $\mu^* = 6$; the numbers alongside the curves designate the magnitude of the parameter M) [8, 59].

resonance scattering, is attained for $A = 10$, $M = 2$. By this means, the $\alpha^2\sigma$ factor may be essentially increased through the agency of resonance scattering at the same chemical potential.

Calculations made on the relationships between $\alpha^2\sigma$ and the chemical potential revealed that $\alpha^2\sigma$ grows with increasing chemical potential at optimal values of the resonance scattering parameters, whereas the dependence of $\alpha^2\sigma$ on μ^* in the presence of normal scattering mechanisms takes the form of a curve with a maximum close to $\mu^* = 0$ [8, 60]. Not only does the inclusion of resonance scattering permit the enhancement of $\alpha^2\sigma$ at fixed μ^*, but it also permits it to be increased with respect to its maximal value corresponding to $\mu^* = 0$.

The optimal value $M = 2$ is consistent with a rather high impurity-band filling with holes ($k_h \approx 0.85$), which can only be attained through additional doping of a sample with an acceptor impurity.

In this manner, double doping offers not only a convenient method of investigating resonance states, but also constitutes a necessary condition for the attainment of elevated thermoelectric figures of merit through the mechanism of resonance scattering.

The inclusion of the resonance scattering of carriers makes it sensible to employ samples with relatively high chemical potentials in thermoelectric devices; these samples evidently possess elevated concentrations of holes in the valence band as well. Electronic contribution to thermal conductivity is correspondingly increased in importance. In the limiting case of high hole concentration, where the electron component of thermal conductivity becomes dominant, the thermoelectric figure of merit defined by Eqn (15) takes the form

$$Z = \frac{\alpha^2}{LT}, \tag{18}$$

where L is the Lorentz number. As computations showed, the Lorentz number is also influenced by resonance scattering with its magnitude being reduced by a factor of 1.65 for

$\mu^* = 6$ and $\Gamma^*/2 = 1$ to result in the relevant enhancement of Z (except for the growth owing to α^2).

Experimental data obtained on Tl- and Na-doped PbTe samples confirmed the conceptions developed above. The samples concurrently doped with 1 at.% Tl and 1 at.% Na exhibited essentially higher thermoelectric efficiency than those doped with identical amounts of Tl and Na separately at the same hole concentration [8].

3.4 Low-temperature anomalies of resistance

In PbTe single crystals alloyed with thallium, Andronik and co-workers [61, 62] revealed anomalies in the behavior of resistance depending on temperature and magnetic field at low temperatures (at around 5–20 K). The temperature dependence of resistivity passed through a minimum whose location was governed by the thallium content (see Fig. 12). For $T < T_{\min}$, the resistivity rose as the temperature decreased. Such a behavior of resistivity is atypical for conventional scattering mechanisms and is observed in degenerate semiconductors, where the Kondo effect shows itself [63, 64].

Of the Kondo effect, negative magnetic resistance is also characteristic; this effect was observed in the sample with 0.5 at.% Tl at the liquid-helium temperature [61, 62]. The resistivity as a function of the magnetic field showed a minimum at a magnetic field induction B of about 1 T. Whilst negative magnetoresistance was not observed in samples with higher thallium contents, the relationship between σ and B differed from the regular dependence.

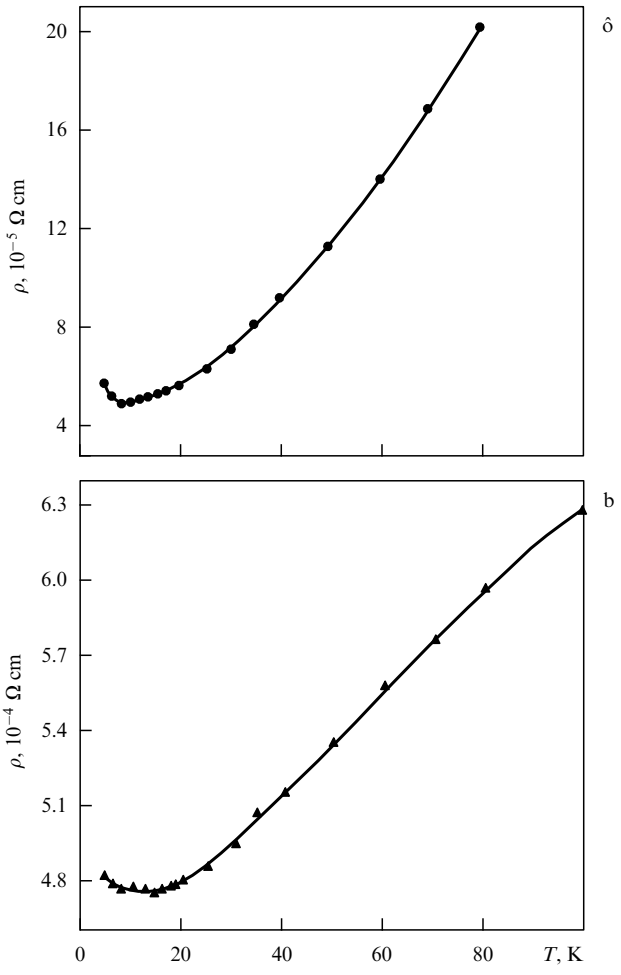

Figure 12. Temperature dependence of the resistivity of PbTe:Tl single crystals at low temperatures [61]: (a) $N_{\mathrm{Tl}} = 0.5$ at.% and (b) $N_{\mathrm{Tl}} = 1.25$ at.%.

The existence of localized magnetic moments [65] giving rise to the Kondo effect was originally associated [61] with the impurity resonance levels of Tl in PbTe. However, measurements of the magnetic susceptibility of PbTe:Tl crystals demonstrated that paramagnetism stemming from localized moments (and, according to the Langevin formula, varying in inverse proportion to temperature) was not found in the crystals under study [66]. The paramagnetic contribution to the magnetic susceptibility takes the form characteristic of Pauli paramagnetism (see below, Section 4.4). Attempts to detect an EPR signal [67, 68] or Schottky anomalies in low-temperature heat capacity (see Section 4.2) in PbTe:Tl samples with various impurity concentrations and degrees of compensation levels came to nothing, also attesting that localized moments are lacking. Observation of superconductivity in PbTe:Tl samples (see below, Section 5) put forward one more argument against the existence of localized moments at Tl impurity atoms in PbTe, because the paramagnetic impurities contribute to the decomposition of a superconducting condensate.

It should also be emphasized that according to Anderson's theory [65], localized magnetic moments occurring in circumstances where strong hybridization of the impurity and band states shows itself require the involvement of prominent repulsive forces between electrons on the impurity center with an energy U in excess of the resonance level broadening. However, experiments on the chemical potential pinning upon double doping (see Section 2.2) demonstrated that the Hubbard energy U is small (or negative). Furthermore, in the sample with a relatively small content of Tl (0.5 at.%), the hole concentration is distinctly lower than the thallium concentration and the Fermi level of electrons lies well above the Tl resonance states. From this it follows that practically all the quasi-levels for such a sample must be occupied by two electrons, eliminating the appearance of localized moments at the thallium atoms.

The lack of localized moments led Andronik [69] to the conclusion that the Kondo-like anomalies of resistance are conditioned by the carrier scattering from two-level centers, which can be described in the quasi-spin language and the scattering from which proceeds analogously to the Kondo effect. The appearance of two-level centers was assigned to the possible noncentral location of impurity atoms. However, a noncentral position about sizable thallium ions also calls for explanation and independent experimental verification.

Relatively low hole concentrations as against N_{Tl} testify that the acceptor action of thallium is partially compensated for by the donor effect of intrinsic defects (the tellurium vacancies, supposedly). Two-level centers were previously discovered and investigated in undoped n-type lead chalcogenides, where chalcogen vacancies created electrons [70–73]. Both the Kondo-like behavior of resistance [70] and the low-temperature heat capacity conditioned by two-level systems (tunnelling states), which were assigned to chalcogen vacancies [71–73], were observed in the experiment. It is conceivable that the presence of tellurium compensating vacancies may account for the Kondo-like resistance anomalies observed in the thallium-doped p-type PbTe samples.

4. Spectroscopy of resonance levels

Although chemical potential pinning upon double doping and resonance scattering are highly probably indicative of the occurrence of resonance states and permit determination of their parameters, it is customary to reason that studies on transport phenomena provide indirect data for the impurity electronic spectrum and that it is desirable to employ more direct methods. There is indubitable reason to think that for every approach we can point out merits and difficulties associated with data interpreting. The body of results obtained by employing a variety of methods allow us to depict a plausible picture of the electronic spectrum with full details. The present chapter deals with the conclusions resulting from the analysis of experimental variables and regularities independent of the charge carrier scattering mechanisms. We set forth the results of investigating radiation absorption (IR spectroscopy), the tunnelling effect in MIS (metal – insulator – semiconductor) structures (tunnelling spectroscopy), the low-temperature heat capacity (calorimetric spectroscopy) and, finally, the magnetic susceptibility.

4.1 Optical absorption

Veĭs and co-workers [5, 6, 28, 30, 33, 34, 74 – 78] began recording the spectra of optical absorption in lead chalcogenides doped with group III elements from the very discovery of the thallium impurity state. These investigations were continued in parallel with measurements on the transport processes. Some additional peculiarities of radiation absorption were revealed in studies of infrared absorption spectra against the fundamental band and of absorption by free holes. These peculiarities were concerned with the transitions between impurity and band states (see Fig. 13) and had the appearance of clearly defined peaks at low hole concentrations, which was achieved either by using small amounts of Tl (0.05 – 0.30 at.%) or by compensation of the thallium acceptor action using an excess of lead. In this case, there are unoccupied electron states in the neighborhood of the valence-band top and optical absorption is controlled by electron transitions from the resonance band to the upper part of the valence band.

Additional absorption peaks in the spectra of thallium-doped samples fell within the frequency range corresponding the energy separation between the valence-band top and the resonance levels discovered by electrophysical methods (see above, Section 2.1), providing direct verification of the thallium resonance state occurrence within the valence band. The energy of resonance states that were determined by optical measurements depended on temperature, hole concentration, and solid solution composition [68, 77, 78]. On the whole, the 'optical' energies ε_i were somewhat higher than the 'thermal' ones derived from the analysis of experimental data on transport phenomena in semiconductors. The Stokes shift observed derives from the fact that due to the Frank – Condon principle, electronic transitions occur without lattice rearrangement, due to changes of the impurity atom charge state. A comparison between the 'optical' and 'thermal' energies of impurity states shows that the Stokes shift in PbTe:Tl is about 60 meV [68], whereas in PbS:Tl it is roughly equal to 100 meV [77].

Apart from absorption peaks pertaining to the Tl resonance band, a complementary absorption was also observed and attributed to electron transitions from quasi-

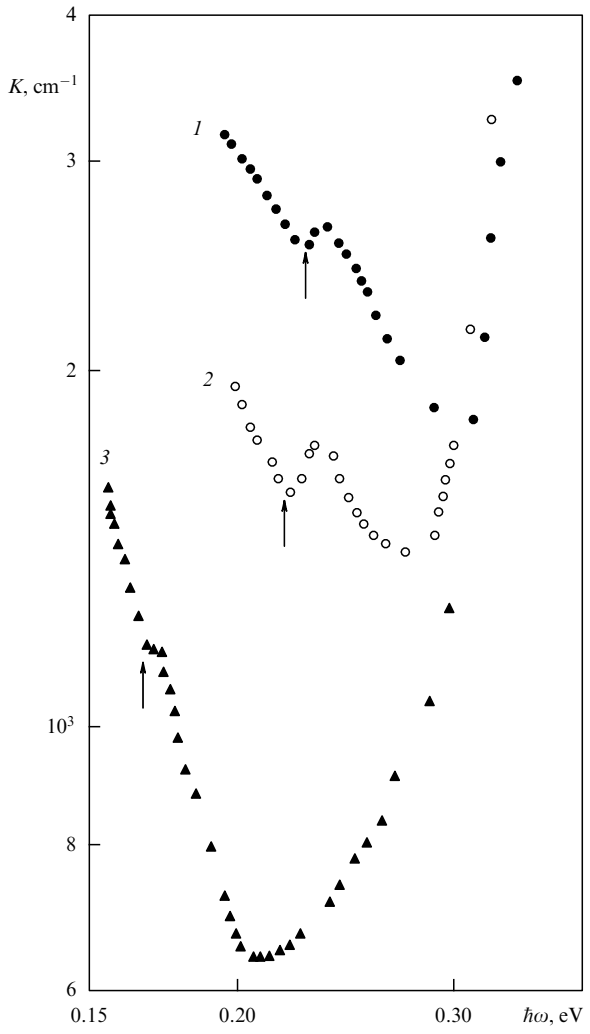

Figure 13. Variation of the absorption coefficient with frequency in PbSe:Tl for $N_{Tl} = 0.5$ at.% and $p = 7.9 \times 10^{18}$ cm^{-3} at various temperatures [28]: (*1*) 473; (*2*) 358; and (*3*) 96 K. The arrows indicate the positions of the 'red' edges of impurity absorption.

local states (created by the Tl vacancies under an excess of Pb) and thermal activation of electrons to localized states in the forbidden band. These latter were ascribed to complexes combining thallium atoms with intrinsic defects [68, 77].

Analysis of the complementary absorption spectrum also furnished a means of estimating the Tl impurity band width in lead chalcogenides. The impurity band in PbTe turned out to be much broader as opposed to the case of two other lead chalcogenides; this presumably occurs as a consequence of the hybridization between the impurity states and the second valence band states of higher density. For instance, the results of the work [74] show that the bandwidth Γ rises from 30 meV to 100 meV with an increase in temperature from 120 K to 300 K. The band is also broadened by three times as the thallium content increases from 0.1 – 0.5 at.% to 1.5 at.% [75].

Of some interest is the dependence of the Tl band width on the composition of $PbSe_{1-x}S_x$ solid solutions [33]. In PbSe and PbS ($x = 0$ and $x = 1$, respectively), the band width at 300 K lies in the range 10 – 20 meV and increases to 60 meV for $x = 0.5$. Fluctuations in the solid solution composition might be supports for explaining the band broadening observed, when it is considered that the position of the

resonance band changes approximately 100 meV in going from PbSe to PbS.

In the thallium-doped $PbSe_{1-x}Te_x$ solid solutions, the position of the band depends only slightly on x, while its width is slow to rise with increasing tellurium content up to $x = 0.8$, following which it grows steeply. It seems likely that this increase is brought about by the transfer of resonance states into the second valence band as the solid solution composition approaches PbTe.

4.2 Low-temperature heat capacity

Measurements of low-temperature heat capacity are one of the most direct investigation techniques concerning an impurity band. The peak in the density of electron states near the middle of the impurity band contributes significantly to the electronic heat capacity, which is observed against the phonon heat capacity in a temperature range of 1 – 4 K. By measuring low-temperature heat capacity, the investigation of thallium resonance states in PbTe was carried out on samples doubly doped with thallium and sodium [79]. The change in the number density of the supplementary Na impurity at fixed (for each series of samples) concentrations of Tl furnished a means for transferring the Fermi level across the impurity band and for determining the density of states as a function of the degree of filling of resonance states. In this manner, the researchers managed to explicitly observe a clearly defined peak in the density of electron states.

The density of states $g(\mu)$ at the Fermi level was determined from the experimental value of the electronic heat capacity C_e by the formula

$$C_e = \gamma T = \frac{\pi^2}{3} k_B^2 T g(\mu) . \qquad (19)$$

Figure 14 presents the resultant curves for the dependence of the density of states on the Na concentration. The curves are bell-shaped with their maxima positioned in the middle of the impurity band. For a thallium concentration of 0.5 at.%, the density of states increases four- to fivefold as the Na content rises to the values corresponding to the position of the Fermi level near the middle of the Tl resonance band. With a further increase in N_{Na}, when the band is emptied at the expense of electrons, the density of states again diminishes practically to the magnitudes found in the absence of Na, i.e., when the impurity band is almost completely occupied with electrons. The density of states for $N_{Na} = 0$, the position of a maximum in the $g(N_{Na})$ curve, and the boundaries of its decay lend credence to the electrophysically obtained total number of states in the impurity band, compatible with two states per Tl atom (see above Section 2.2).

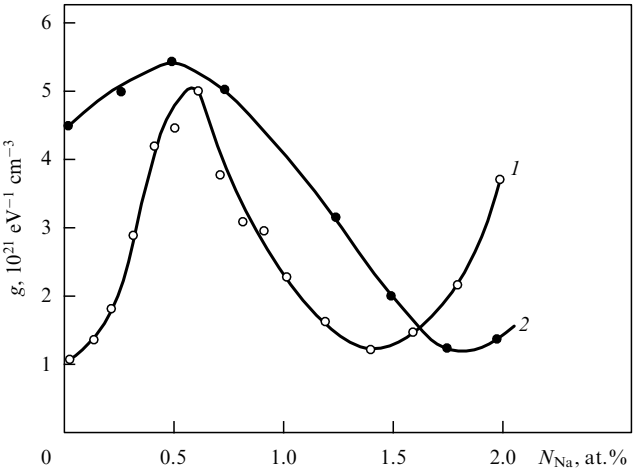

Figure 14. Density of states at the chemical potential level versus the amount of additional Na acceptor impurity in PbTe:Tl [79]: (*1*) $N_{Tl} = 0.5$ and (*2*) — 1.25 at.%.

For samples with the sodium concentration at which the electronic heat capacity has a maximum, the Hall concentration of holes $p \approx (5-7) \times 10^{19}$ cm^{-3} is appropriate to the Fermi level $\varepsilon_i \approx 0.2$ in full compliance with the electrophysically determined 'thermal' energy of the thallium states.

Estimating the resonance band width by the formula

$$\Gamma \approx \frac{2N_{Tl}}{g_{max}} \qquad (20)$$

yielded the magnitude $\Gamma \approx 30$ meV for $N_{Tl} = 0.5$ at.%. As Fig. 14 suggests, the maximal value of the density of states grows almost not at all with increasing thallium content, in spite of an appreciable gain in the total number of states in the band. By this is meant that the band width rises more than twofold with increasing N_{Tl} up to 1.25 at.% in agreement with optical data (see Section 4.1).

The increase in Γ may be linked to variations in the impurity band position under conditions of strong hybridization of impurity and band states. As is shown in Ref. [32], with rising thallium content, the impurity band shifts into the valence band. This shift is relatively insignificant (see Section 2.3) but taking into account the proximity of resonance levels to the edge of the second valence band, it can be inferred that with an increase in N_{Tl}, the levels can meet the edge of the second valence band and go deep into this band. A fast increase in the density of band states, against whose background the resonance band is positioned, could affect the band broadening on account of hybridization.

The gain in Γ with increasing temperature may also be ascribed to the same cause. This gain was obtained from the analysis of optical data at temperatures approaching 100 – 300 K and from comparison with the results on low-temperature heat capacity as well. Referring to electrophysical measurements, the Tl resonance band nears the band edge of light holes more slowly than the second extremum of the valence band and hence with rising temperature the impurity band can go deeper into the second valence band.

In studies of low-temperature heat capacity, multiple attempts were made in an effort to discover Schottky anomalies stemming from the impurity level splitting in a magnetic field. The negative result evidences the lack of localized magnetic moments at the Tl impurity atoms. Hybridization of the impurity and band states at a small (as compared to Γ) or negative correlation energy U is likely to clarify the last circumstance.

The results of low-temperature heat capacity measurements on PbTe samples alloyed with Tl and In demonstrated qualitative distinctions in the behavior of these group III-element impurities. Despite the high density of In quasi-local states in PbTe, no peak of heat capacity was detected, which is explained by long-term relaxation of the In charge state (see Section 2.1).

4.3 Tunnelling spectroscopy

Information on the density of electron states in semiconductors, including the density of impurity states, can also be obtained from an analysis of current – voltage characteristics

of tunnelling MIS structures. Tunnelling spectroscopy has the advantage that the impurity band probing is effected by way of variation of the bias voltage V across a sample without changing the content of a particular dopant.

Single crystals of PbTe were the subject of investigation by tunnelling spectroscopy in Ref. [80]. They contained various impurities and defects, among them 0.2 at.% Tl. Tunnelling MIS contacts $Pb-Al_2O_3-PbTe$ were fabricated and then employed in measuring and analyzing the differential conductivity $\sigma(V) = dI/dV$ of MIS structures as well as its derivative $\sigma'(V) = d^2I/dV^2$ with respect to voltage. The resulting dependences $\sigma(V)$ and $\sigma'(V)$ exhibited a series of peculiarities conforming to those in the electronic spectrum, such as the valence band extrema and the Tl impurity band. By this means, a certain pattern of electronic spectrum was peculiar to the current–voltage characteristic. Figure 15 displays a fragment of the tunnelling spectrum possessing a number of salient features which are of most spectroscopic interest in the Tl impurity states. The abscissa was the hole energy reckoned from the top of the valence band. The curve $\sigma(\varepsilon)$ has a peak at $\varepsilon = \varepsilon_i$, which is only present for thallium doping and correspond to the peak of the density of thallium resonance states. A bend in the $\sigma(\varepsilon)$ curve at $\varepsilon = \varepsilon_{v2}$ was observed in all the structures at hand irrespective the sort of impurity and the degree of PbTe doping; it was interpreted as a manifestation of the maximum of the second valence band.

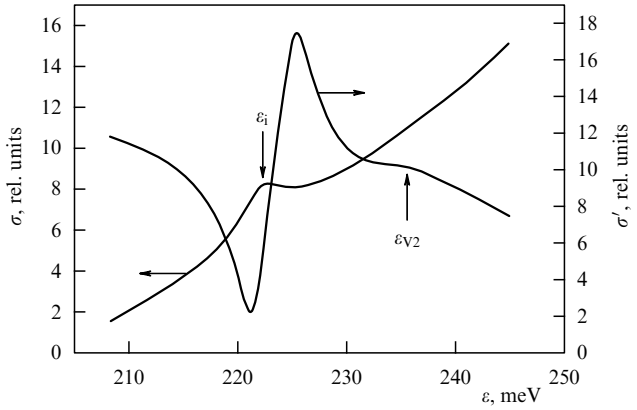

Figure 15. Fragment of the tunnelling spectrum for a PbTe single crystal doped with 0.2 at.% Tl [81].

Analysis of the tunnelling current–voltage characteristics discloses that the center of the peak of impurity states is located near the edge of the second valence band (0.013 eV above the edge) in good agreement with electrophysical and optical data.

The shape of the peak is closely described by the Lorentzian (5) with width $\Gamma \approx 4$ meV. This value is smallest amongst all those derived by various methods for the PbTe:Tl samples. At least partly it is owed to the fact that the tunnelling spectra were taken at liquid-helium temperatures and a relatively small content of Tl, whereas the width Γ, as discussed above, showed an increase with rising temperature and thallium concentration.

In such a manner, tunnelling spectroscopy permitted the production of direct evidence for the presence of thallium resonance levels in the valence band. A crystalline sample with a relatively low impurity content served as the subject of inquiry, so that the Fermi level lay above the impurity level, i.e., the impurity states were fully filled with electrons.

An essential difference in the properties of two doping elements – thallium and indium – from group III of the periodic table shows up in both the tunnelling characteristics of MIS structures and the low-temperature heat capacity. Although doping lead telluride with indium brings about an extremely hard pinning of the Fermi level in the neighborhood of the conduction-band edge, no peaks of $\sigma(V)$ in the relevant portion of the current–voltage characteristic were observed in the PbTe:Tl-based MIS structures. Instead, indium doping affects the hysteresis on reversal of the voltage sweeping over the range of V variation from -50 to 50 mV [80, 81]. The hysteresis is indicative of the existence of metastable states originating in the In impurity. The hysteresis effect was interpreted with the hypothesis that upon changes in the charge state of the center, a local rearrangement of the crystal lattice containing the impurity atom occurs.

4.4 Magnetic susceptibility

Magnetic susceptibility was measured as a function of temperature and charge carrier concentration in single-crystal lead telluride doped with thallium in amounts from 0.1 to 1.3 at.% at temperatures of 77–280 K [66]. The total magnetic susceptibility measured turned out to be diamagnetic and on subtracting terms independent of the hole concentration, one was left with a hole contribution characteristic of Pauli paramagnetism. The magnitude of such contribution rose sharply with an increase in the hole concentration beyond $\sim 5 \times 10^{19}$ cm^{-3}. This concentration is appropriate to the onset of filling of the thallium impurity band with holes, which explains the threshold behavior of the concentration dependence of the magnetic susceptibility.

The density of impurity states of the Fermi level was evaluated with the Pauli formula [66]. For $p \approx 7 \times 10^{19}$ cm^{-3}, at $T = 80$ K, in particular, the density of states was $g \approx 2 \times 10^{21}$ eV^{-1} cm^{-3} at a resonance band width of about 10–60 meV, which agrees with the results obtained by other methods (see Sections 3.2, 4.2 and 5).

5. Superconductivity

5.1 Superconductivity of thallium-doped PbTe

When examining the temperature dependence of heat capacity in PbTe:Tl for the purpose of studying resonance states, the authors of Refs [52, 82] revealed the presence of a peak in a temperature range between 1 and 1.5 K (see Fig. 16), which was interpreted merely as a somewhat smeared (within the interval ~ 0.1 K) heat capacity jump characteristic of the second-order phase transitions. Detailed analysis of the data led the authors of Refs [82–85] to the unambiguous conclusion that this jump is due to the transition to a superconducting state at a critical temperature $T_c = 1.4$, which is extraordinarily high for semiconductors. Several experimental facts and regularities are listed below, which in aggregate allow us to conclude that the effect under observation corresponds to a transition to the state of type II bulk superconductivity.

Figure 16 displays the hole heat capacity $C(T)$ in the thallium-doped PbTe sample, which is compared with the relevant curve $C_0(T)$ for an undoped sample with a low hole concentration; this latter curve exhibits no peculiarities. The

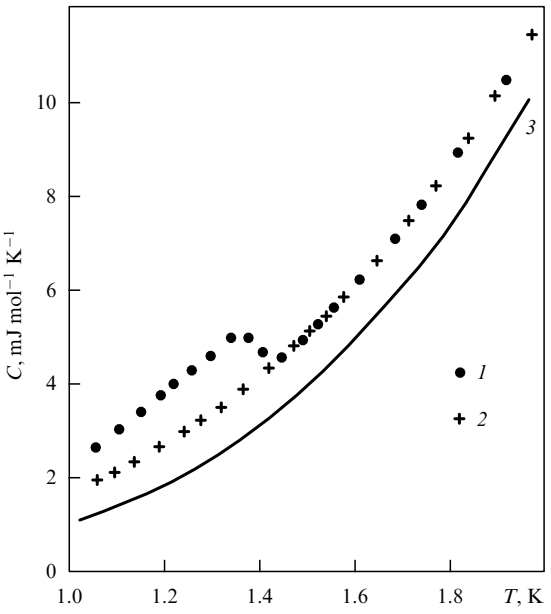

Figure 16. Temperature dependence of the molar heat capacity C of the PbTe:Tl sample with $N_{Tl} = 1.5$ at.% at low temperatures [83]. The magnetic field strength H, kOe: (*1*) 0; and (*2*) more than 2.5; line *3* was constructed from data for undoped PbTe.

magnitude of the jump in the $C(T)$ curve is on the order of the difference between C and C_0, i.e., on the order of the hole heat capacity. This means that the phase transition occurs in an electron subsystem. The magnetic field above $H \approx 2.5$ kOe (at $T = 1$ K) suppresses the effect, which is typical of superconductivity. The magnitude of the jump ΔC proved to be close to the value of the electronic heat capacity C_n in the normal state, i.e., it was in reasonably good agreement with theoretical expectations for a Fermi gas with attractive forces between particles

$$\Delta C = 1.43 C_n(T_c)\,. \tag{21}$$

In the course of measuring heat capacity as a function of temperature and magnetic field intensity, cooling of the sample, i.e., a negative magnetocaloric effect, was observed upon adiabatic magnetization [83]. The magnitude of the effect reduced steeply around $T \approx T_c$, where decomposition of the superconducting condensate by the magnetic field occurred. The large magnitude of the magnetocaloric effect observed in the fields substantially weaker than the upper critical field H_{c2} (where a superconductor undergoes transition to the normal state), testifies to the magnetic field penetration into the sample and serves as evidence that PbTe:Tl is a type II superconductor.

The validity of the inference about superconductivity in PbTe:Tl is strengthened by the fact that it was originally established by measuring the heat capacity of the sample. This measurement procedure was not concerned with the flow of electric current and was insensitive to the sample structure. Prior to publication of the papers considered, a number of reports were given about superconductivity in PbTe [86 – 89] identified from an electrical resistance jump or from magnetic field expulsion (the Meissner effect). However, bulk superconductivity was observed in none of these works: only threads or interlayers of a second phase were superconductive, while surface inclusions of a second phase could screen from magnetic field the interiors of the grains or the sample as a whole. In this respect, it is essential that Pb and Tl entering into the composition of PbTe:Tl are superconductors with transition temperatures of a few degrees. Thus, it is only the calorimetric approach that permits reliable identification of bulk superconductivity in these compound semiconductors. The presence of a jump in the temperature dependence of heat capacity led to the conclusion about the occurrence of superconductivity with a transition temperature of up to 0.2 – 0.3 K in SnTe, GeTe, $SrTiO_3$ and some other semiconductors.

Although electrical measurements alone are not ample evidence for the presence of bulk superconductivity in semiconductors, they are, of course requisite for the final inference that the superconducting transition really occurs in the samples under study. Direct measurements of the temperature dependence of electrical resistivity ρ in PbTe:Tl revealed a jumplike variation at $T = T_c$ by no less than 2 – 3 orders of magnitude up to the level corresponding to the limiting accuracy of measurements [82, 83] (see Fig. 17). The resistance jump was suppressed by the magnetic field H_{c2}, much like the heat capacity jump.

For reducing the temperature-dependent upper critical field H_{c2} to the limit of $T = 0$, the following empirical expression was invoked [90]:

$$H_{c2}(T) = H_{c2}(0)\left[1 - \left(\frac{T}{T_c}\right)^2\right], \tag{22}$$

which yielded $H_{c2}(0) \approx 5$ kOe exceeding (like T_c) the relevant values for other known superconducting semiconductors by an order of magnitude. (The derivative $|\partial H_{c2}/\partial T|_{T_c} = 2H_{c2}(0)/T_c$ may be used for a characteristic of superconducting transition rather than an extrapolated magnitude $H_{c2}(0)$).

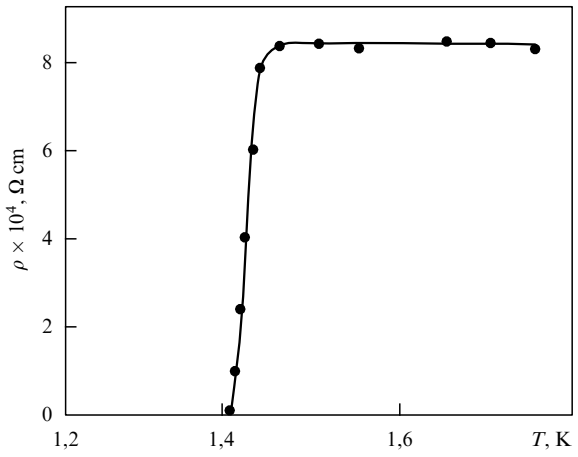

Figure 17. Plot of resistivity ρ in PbTe:Tl with $N_{Tl} = 1.5$ at.% at low temperatures [83].

The formulas developed in the Ginzburg – Landau theory of superconductivity [91] permitted the authors of Refs [82, 83] to evaluate the typical parameters of the superconducting state in PbTe:Tl. One of the major such parameters is the temperature-independent dimensionless Ginzburg – Landau parameter $\varkappa$, which is the ratio between the London penetration depth $\delta(T)$ and the correlation length $\xi(T)$ for

the order parameter. Based on experimental values of the upper critical field H_{c2} at $T = 1$ K and the heat capacity jump $\Delta C(T_c)$, the authors of the works cited above arrived at a magnitude $\varkappa \approx 80$, which appeared to be extremely high for semiconductors. Large values of the Ginzburg–Landau parameter signify that type II superconductivity is involved. An appraisal of the lower critical field H_{c1} bounding the domain of mixed superconductivity from below provided a rather small magnitude of $H_{c1}(1\,\mathrm{K}) \sim 0.1$ Oe, so that direct measurement of H_{c1} presents difficulties; that is why it has not yet been conducted. Finally, theoretical estimation of the Landau–Ginzburg coherence length $\xi(T)$ from the magnitude of H_{c2} yielded the value $\xi(1\,\mathrm{K}) \approx 3.5 \times 10^{-6}$ cm, from which it follows (with allowance for the value of $\varkappa$) that the penetration depth is $\delta(1\text{ K!}) \approx 3 \times 10^{-4}$ cm.

Measurements of the temperature dependence of electrical resistance (bounded from below by a temperature of 0.4 K) in combination with studies of heat capacity at $T \geqslant 1$ K permitted determination of the transition temperature T_c as a function of the Hall concentration of holes p [85]. It was found that contrary to other superconducting semiconductors, the function $T_c(p)$ in PbTe is a prominent example of a threshold function with a threshold approaching $(5-6) \times 10^{19}$ cm^{-3}. This function correlates with the appropriate dependence of the electronic heat capacity proportional to the density of states, which in turn is mainly determined by resonance states in the PbTe:Tl samples at concentrations above 5×10^{19} cm^{-3}. The regularity revealed suggests that resonance states play a crucial role in the origin of superconductivity seen in semiconducting IV–VI compounds [84]. Such a conclusion was supported by investigations (see below Section 5.2) of superconductivity in samples with double doping.

A similar situation holds when the effects of hydrostatic compression on the superconducting transition parameters were studied in thin-film PbTe:Tl samples [36]. The transition temperature T_c decreased from 1.4 to 1.0 K with an increase in pressure from 2 to 7.5 kbar, which was attributed to a displacement of the resonance levels into the depth of the valence band in close agreement with the results on the Hall effect (see Section 2.2) and the enhancement of energy separation between the middle of the impurity band and the Fermi level.

In closing the present section, we compare the superconducting properties of the IV–VI compound semiconductors alloyed with two different elements (Tl and In) of group III of the periodic table. Unlike the thallium dopant, no evidence of superconductivity was found when doping PbTe with indium. But on replacement of a sufficient amount of lead by tin, when the impurity In levels find themselves within the valence band and resonance scattering occurs, superconductivity appears, with a transition temperature even higher than in PbTe:Tl, reaching the value $T_c \approx 4$ K. In such a manner superconductivity and resonance scattering in IV–VI compound semiconductors take place simultaneously under circumstances where impurities of group III elements generate resonance states against the valence band.

5.2 Superconductivity in doubly doped PbTe

The experimental studies of superconductivity in PbTe:Tl described above allow us to hypothesize that the occurrence of this phenomenon depends upon the Tl resonance states [84], though reserving the possibility of other explanations [52]. Experiments on samples of lead telluride alloyed with thallium and some additional dopant modifying the degree of impurity-band filling leave slight doubts about the decisive role of resonance states in the occurrence of superconductivity. Measurements of the temperature dependence of the electrical resistance made on a great number of samples by Parfen'ev et al. [36, 37, 41, 55] and confirmed by the results of measuring heat capacity [93] showed that superconductivity is only observed in circumstances where the Fermi level 'is creeping in' to the impurity band from below or from above. As in the case of studying transport phenomena, sodium [36, 37, 93], lithium [41] and hyperstoichiometric lead [43] were used as an additional dopants.

As noted above (Sections 2.3, 4.2), variations in the concentration of additional impurity at a fixed content of the Tl atoms forming impurity levels make it possible to move the Fermi level across a nearly unchanged impurity band and to probe the density of states as a function of energy. The formulas for superconductivity valid for large values of the Ginzburg–Landau parameter [90] permit us to relate the upper critical field $H_{c2}(0)$ and transition temperature T_c to the density of states $N(0)$ at the Fermi level (per single orientation of spin, as opposed to the above-used quantity $g(\varepsilon)$)[37]:

$$N(0) = 4.8 \times 10^{14} \frac{H_{c2}(0)}{\rho T_c}\,, \tag{23}$$

where the residual resistivity ρ in the normal state was expressed in Ω cm, the upper critical field H_{c2} in Oe, and the density of states $N(0)$ in eV^{-1} cm^{-3}. Measurements of quantities on the right-hand side of Eqn (23) supply a further independent method of determining the density of resonance states; the results are in close agreement with those obtained by the approaches mentioned above, in particular, by calorimetry (see Section 4.2).

Figure 18 gives the dependences of four different quantities on the filling factor (1): the transition temperature T_c, the upper critical field H_{c2}, the resistivity ρ, and the density of states $N(0)$ derived from Eqn (23). These quantities have maxima near $k_h = 0.5$. At the maximum, one finds $T_c = 2.2$ K and $H_{c2}(0) \approx 13$ kOe, i.e., additional doping with acceptors provides a way of increasing the transition temperature and critical field. All four dependences are bell-shaped and closely correlate with each other and with the function for the density of states derived from measurements made in the normal state. An agreement between the density of pairing electrons and that of resonance states, the latter exceeding the density of valence band states by an order of magnitude, bears witness to the fact that electrons in the hybridized states (mainly in the impurity states) participate in pairing and come into play in superconductivity. The agreement between the parameters of superconductivity and the density of resonance states is direct evidence that the nature of superconductivity in PbTe:Tl is closely linked to resonance states.

The regularities obtained signify the presence of a positive correlation between superconductivity and resonance scattering: the enhancement of resonance scattering is accompanied by an increase in the superconducting parameters T_c and H_{c2}. Such a correlation is borne out by the results of studying solid solutions described in the section that follows, as well as by a comparison between PbTe:Tl and thallium-doped PbSe and PbS, where superconductivity has not been detected.

Although the bell-shaped curves portraying the dependences of various variables on the filling factor coincide

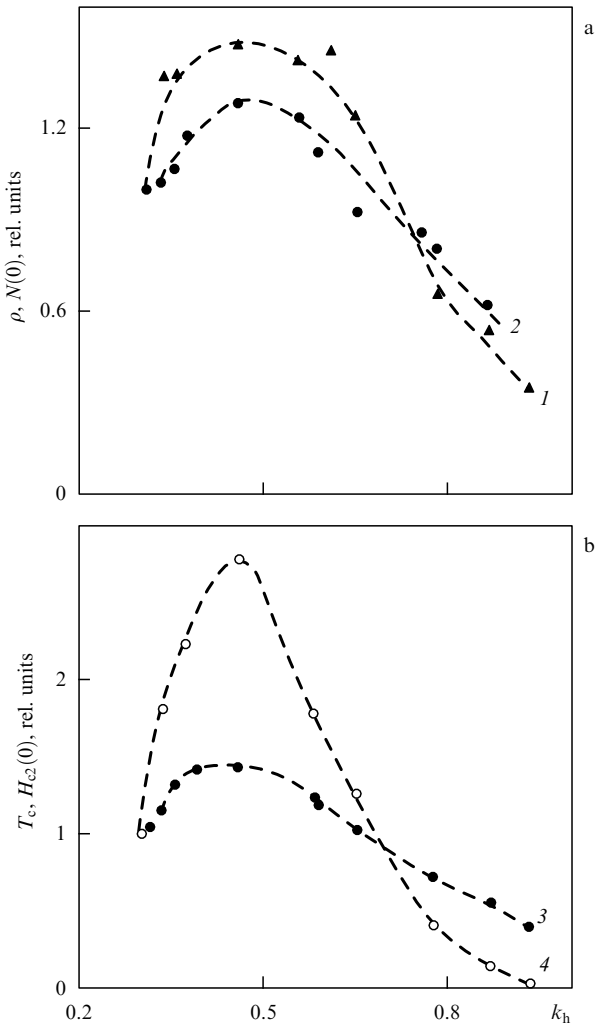

Figure 18. Plots of resistivity ρ (a, curve *1*), density of states at the Fermi level in the normal state $N(0)$ (a, curve *2*), transition temperature T_c (b, curve *3*), and upper critical field $H_{c2}(0)$ (b, curve *4*) in PbTe:(Tl, Na) versus the factor of resonance-band filling with holes. The results are expressed in relative units (data for PbTe:Tl were taken as unit ones) [37]; $N_{Tl} = 2$ at.% in all samples.

principally, a pronounced difference is found in the behavior of the parameters obtained through measurements in the superconducting and normal states. This difference, first detected in measuring electrical resistance [37] and confirmed by the heat capacity method [93], is observed over the interval of the k_h variation corresponding to a drop in the density of states with increasing k_h (or N_{Na}). It turns out that the bell-shaped density of states $g(k_h)$ (deduced from heat capacity measurements) is undistorted and passes through a single maximum near $k_h = 0.5$, whereas the curve $T_c(k_h)$ has two maxima, of which the first practically coincides with the maximum of $g(k_h)$, and the second falls on the descent of the peak that corresponds to $k_h > 0.5$. The nonmonotonic character of the T_c variation with its minimum at relatively large degrees of impurity-band filling with holes has no parallel in other superconducting semiconductors and has not yet been explained theoretically.

Thus, analysis of the available experimental data permits a unique inference to be made about the linkage between the superconductivity observed and the resonance states along with the determination of phenomenological parameters from the Ginzburg – Landau theory. However, at the present time an extended comparison between observational data and theoretical expectations based on a particular variant of microscopic theory of superconductivity is lacking. Here mention may be made of several theoretical works [94 – 99] wherein superconductivity has been linked to resonance states. The negative correlation energy U of electrons in the quasi-local states is of primary importance in the majority of these papers [94 – 98]. The existence of a negative energy U being no more in modulus than the resonance band width is consistent with the above-mentioned results of studying PbTe:Tl in the normal state. In Ref. [99], the superconductivity mechanism was associated with mutual induction of superconducting order parameters in heavy and light subsystems (electrons occurring in the quasi-local and band states). A choice of microscopic theory adequate to the body of experimental data at hand and determination of its parameters is a problem for later studies.

5.3 Superconductivity in PbTe-based solid solutions

Research of thallium-doped solid solutions of IV – VI compound semiconductors in the normal state (see Sections 2.2, 4.1) showed that a partial replacement of the Pb and Te atoms as well as changes in the solid-solution composition significantly affects the parameters of resonance states. Studies of superconductivity in solid solutions are aimed at elucidating the behavior of superconducting transition parameters under these variations. The solid solutions with a replacement of Pb, Te atoms in both the sublattices have been the subject of extensive research: $Pb_{1-x}Sn_xTe$ [100], $Pb_{1-x}Ge_xTe$ [101, 102], $Pb_{1-x}Si_xTe$ [102], $PbTe_{1-x}Se_x$ [103], and $PbTe_{1-x}S_x$ [104].

It has been found experimentally that substitution of the lead and tellurium atoms gives rise to essentially different changes in the superconductivity parameters. With tin in place of lead, the parameters T_c and $|\partial H_{c2}/\partial T|$ of the superconducting transition decline rapidly with increasing content of tin despite a rise in the hole concentration, so that the samples with $x = 0.03$ do not change to the superconducting state even for $T = 0.07$ K. Replacement of lead with other group IV elements, e.g., Ge or Si, has an even stronger negative impact on superconductivity. The higher the position of the element in the periodic table, the smaller its content at which superconductivity dies out. On substitution of selenium or sulfur for tellurium, the magnitudes of T_c and $|\partial H_{c2}/\partial T|$ vary only slightly right up to 5 at.% Se and 10 at.% S.

Variations seen in the parameters of superconducting solid solutions correlate with the peculiarities of their compositional influence on the band parameters of the thallium resonance states (see Section 2.2). On substitution by chalcogenes, the energy position and width of the band change weakly with the composition variations. In a $Pb_{1-x}Sn_xTe$:Tl solid solution, the impurity band goes deep into the heavy-hole band, while the Fermi level escapes from the band, the width of the band enhances, and the density of resonance states at the Fermi level decreases, thus resulting in a fast decrease in the superconductivity parameters. The observed correlation between the properties of samples in the normal and superconducting states served as another argument in favor of the inference that resonance states are crucial for superconductivity occurring in semiconductors based on PbTe:Tl.

Considering thallium to be an impurity that substitutes for lead in PbTe, the results of superconductivity research in

solid solutions testify to a strong localization of the Tl impurity states and to a decisive role of the metal sublattice in their formation.

It must be added that a softening of the optical phonon mode with a rise in x in the $Pb_{1-x}Ge_xTe$ solid solutions [101] produces no positive effect upon their superconducting properties; even small Ge admixtures cause the superconductivity to die out.

The order–disorder type of phase transition observed in $PbTe_{1-x}S_x$ solid solutions for $x \geqslant 0.02$ [105] also leaves the superconducting transition practically unaffected.

6. Self-compensation in thallium-doped lead chalcogenides

The essence of the self-compensation phenomenon is that on introducing electrically active dopants to a sample, the formation of intrinsic lattice defects becomes energetically advantageous. These defects give rise to charge carriers of opposite sign and as a consequence, the donor or acceptor action of the dopant substantially decreases.

The physical nature of self-compensation is as follows. Let us suppose that the semiconductor was strongly alloyed with an electrically active dopant (for the sake of definiteness, an acceptor-like dopant, like thallium in lead chalcogenides) which in the absence of impurity levels and compensating defects would have created holes in the valence band with a concentration appropriate to the density of acceptors. If the intrinsic defects possessed donor properties, their formation in the absence of acceptors would have given rise to electrons in the conduction band. Recombination of holes and electrons created by the impurities and defects, respectively, lowers the system energy per single electron–hole pair by a magnitude of the order of the forbidden band width ε_g. This energy gain will cause the vacancy concentration to increase during the establishment of thermodynamic equilibrium and thus the acceptors to be compensated for by donor defects. The phenomenon described is generally referred to as self-compensation [106, 107] because it is precisely this electrically active effect of the impurity (thanks to statistical interaction between the impurity and the defects through the mediation of an electron subsystem) that is responsible for the appearance of an additional number of compensating defects.

Self-compensation for the acceptors in the 'relatively-narrow-gap' lead chalcogenides is clearly observed in circumstances where a sizable excess of lead is present in the samples at hand. Here, we are concerned with the most interesting case of maximal self-compensation.

An investigation of the maximal self-compensation in IV–VI compounds turned out to be closely related to explorations into quasi-local states created by the impurity group III elements. Both the self-compensation and resonance states can essentially reduce the electrically active effect of the impurity by lowering the concentration of free carriers created. Alternatively, theoretical examination of the self-compensation observed demonstrated that to account for the density of resonance states affects the steady-state concentration of compensating defects. Finally, new localized and resonance states, which can be created by both the impurities and defects, were observed in the compensated samples where the chemical potential is found within another energy range compared to the uncompensated samples.

6.1 Self-compensation of the thallium effect in PbSe

The thallium-doped lead selenide turned out to be the first IV–VI compound in which the maximal self-compensation was studied and through the agency of the latter, samples were fabricated with a rather low concentration of electrons and holes and a large density of impurities and defects [108, 109]. PbSe samples with a thallium concentration N_i of up to 0.8 at.% were produced by the method of hot pressing followed by annealing at a temperature of 650 °C for 100 h.

The charge carrier concentration was determined by measuring the Hall coefficient. The sign and magnitude of the Hall constant showed that at large excess of lead the samples at hand possessed both n-type and p-type conduction depending on the thallium content N_i. The charge carrier concentrations were more than an order of magnitude below N_i.

To determine the sample composition at which maximal self-compensation occurred, the dependences of the charge carrier concentration on the excess of lead in reference to the quasi-stoichiometric composition (corresponding to the chemical formula $Pb_{1-x}Tl_xSe$) were first measured at fixed thallium content. The introduction of excess lead gives rese to a reduction in the hole concentration; the type of conduction changed at a thallium content of up to ~ 0.24 at.% and a sufficiently large lead excess. At an excess of lead approaching $(0.5-0.8)N_i$, the curve under consideration showed a bend and the charge carrier concentration as a function of excess lead exhibited saturation, having suggested that the homogeneity-range boundary was reached from the excess lead side and maximal self-compensation occurred.

At the temperature of the Hall coefficient measurements, the charge carrier concentration is large in comparison with the intrinsic concentration n_i and hence the concentration difference of holes and electrons $p - n$, which is calculated in the following, practically coincides with the measured values of p in the p-type samples and with those of $-n$ in the n-type samples. The quantity $p - n$ corresponding to maximal self-compensation is plotted against N_i in Fig. 19. It is obvious from the figure that the change in the conduction type for maximally compensated samples comes about at $N_i \approx 0.24$ at.% ($\sim 4 \times 10^{19}\,cm^{-3}$). The carrier concentrations are of the order of $(1-3)\times 10^{18}$ cm^{-3}, which is more than an order of magnitude below N_i. The lowest Hall concentration of 4×10^{16} cm^{-3} was obtained at a Tl content approaching the point of conduction type change, i.e., the point of complete self-compensation $N_i = N_i^*$.

The experimental data obtained were attributable to self-compensation of acceptors by isolated point defects (vacancies). When interpreting the experimental findings, the theory of self-compensation developed in Refs [108, 109] based on the minimization of thermodynamic potential was employed. The condition of minimum of the thermodynamic potential, along with the condition of neutrality and the appropriate equalities descriptive of the linkage between the concentrations of electrons and holes and the chemical potential μ, allowed an exact analytical solution to the system of equations and the relationship between the acceptor concentration and the quantity $p - n$ to be obtained which is temperature-independent at the 'frozen' vacancy concentration and can be measured using the Hall effect.

Figure 19 depicts the theoretical curves for the concentration difference $p - n$ as a function of N_i in circumstances where compensation by single- and double-charged vacancies takes place. The theory agrees nicely with experimental results

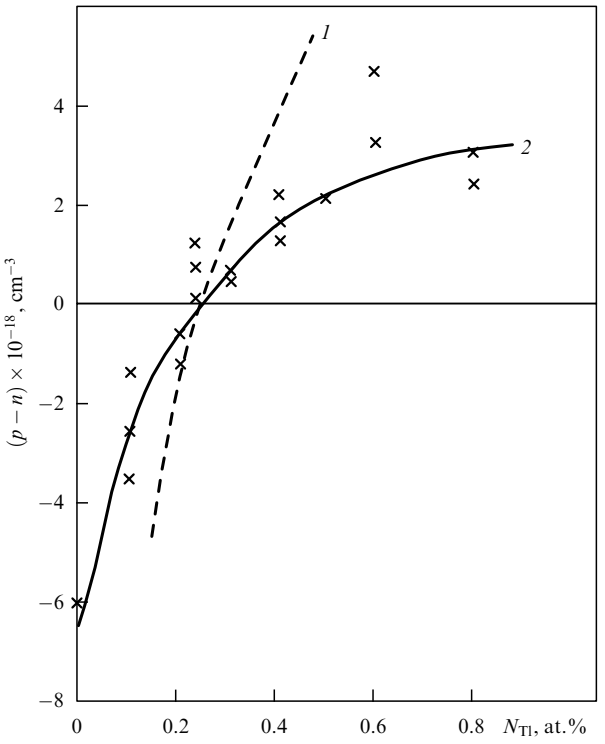

Figure 19. Plot of difference $p - n$ between the concentrations of holes and electrons versus thallium content N_{Tl} in PbSe:Tl samples in equilibrium with the lead phase [108]. The lines were calculated: (*1*) for thallium compensated by singly ionized lead vacancies; (*2*) the same but with doubly ionized lead vacancies. The points designate experimental data.

on the assumption that each vacancy produces two electrons (compensates for two holes).

The curves displayed in Fig. 19 were constructed with a single adjusting parameter N_i^*. However, this parameter can be calculated using the electron concentration corresponding to the boundary of the homogeneity range from the excess lead side in undoped samples at the annealing temperature. The calculations done in Refs [108, 109] brought the computed value of the parameter into coincidence with the measured value with an accuracy of 10%, so that computational curves in Fig. 19 may be thought of as having been constructed without a particular adjusting parameter if one leans upon the known phase diagrams for the undoped lead selenide.

Given the parameter N_i^*, the enthalpy of vacancy formation in PbSe can be calculated [108, 109]. It was found to be approximately 0.9 eV at a temperature of 650 °C.

Self-compensation should be considered as strong if the change in the charge carrier concentration proves to be small in comparison with the variation of the doping admixture content, i.e., if the derivative $\partial(p-n)/\partial N_i$ is reasonably small. For strong compensation, straightforward formulas governing the dependence of $(p - n)$ on N_i were obtained [108, 109]. In particular, for doubly charged vacancies, one obtains

$$p - n = n_i \frac{N_i - N_i^*}{\sqrt{N_i N_i^*}}, \tag{24}$$

where n_i is the intrinsic concentration of charge carriers at the annealing temperature. Taking the derivative of Eqn (24) with respect to N_i at point $N_i = N_i^*$, one can readily see that the condition for strong self-compensation reduces to the smallness of the parameter

$$\delta = \frac{n_i}{N_i^*}. \tag{25}$$

To calculate the self-compensation parameter δ, the concentrations N_i^* and n_i have to be evaluated. In order that n_i be computed, one needs to know the integrated densities of states N_c and N_v for the conduction band and valence band, respectively, with account made for the second valence band and the band of thallium impurity states when evaluating the latter quantity. The effective value of N_v may be presented as

$$N_v = N_{v1} + N_{v2} \exp\left(-\frac{\Delta\varepsilon_v}{k_B T}\right) + 2N_i \exp\left(-\frac{\varepsilon_i}{k_B T}\right). \tag{26}$$

Calculation of δ with due regard for Eqn (26) at $T = 923$ K yields 0.13, i.e., $\delta \ll 1$, verifying the possibility of strong self-compensation of acceptors in PbSe by simple point defects.

6.2 Self-compensation in PbTe:Tl

Computation of the self-compensation parameter δ in PbTe using the phase diagram of undoped crystals yields the values $\delta \gg 1$ in circumstances where acceptors are compensated by vacancies or other isolated point defects over a wide range of temperatures [109], i.e., self-compensation of acceptors by ordinary defects cannot occur in lead telluride. The reason for the high magnitudes of the self-compensation parameter δ is that for the high annealing temperatures, at which the steady-state concentration of defects is reached, the forbidden band in PbTe (bounded by the top of the band of heavy holes) is found to be markedly narrower, and hence the intrinsic carrier concentration n_i is higher than in PbSe and PbS.

In the mean time, experimental studies have shown that strong self-compensation of the Tl acceptor action is observable in PbTe with excess lead [110]. Under the conditions of maximal self-compensation, the hole concentration retained its constant value in the neighbourhood of 4×10^{18} cm^{-3} over a wide range of variation of thallium impurity content from 0.1 to 2 at.% ($1.5 \times 10^{19} - 3 \times 10^{20}$ cm^{-3}).

Strong self-compensation for the Tl effect in PbTe, as well as for other donors and acceptors in PbTe, was associated with the formation of impurity – vacancy complexes. The existence of the binding energy for a complex reduces the total energy of defect production and in doing so it aids increasing concentration of compensating defects, opening the way to strong self-compensation in those cases where formation of a sufficient amount of ordinary defects is energetically disadvantageous. The inclusion of the contribution from complexes to the thermodynamic potential tangibly affects the dependence of the charge carrier concentration on the impurity content N_i under the conditions of maximal self-compensation [109, 111, 112]. In particular, saturation of the quantity $(p - n)$ is attained for compensation by pair complexes in the limit of large N_i, whereas according to Eqn (24) one has $p - n \sim N_i^{1/2}$ for compensation by simple defects. The clearly pronounced saturation of the $p - n$ dependence on N_i in PbTe:Tl, along with strong self-compensation at high calculated values of the self-compensation parameter δ, was the basis of invoking the mechanism of complex formation when interpreting experimental data available.

6.3 Self-compensation in PbS:Tl

Based on the low theoretical values for the self-compensation parameter δ in PbS:Tl ($\delta \approx 0.006$ for PbS with acceptors and excess lead at a temperature of 650 °C [109]), a stronger self-compensation for Tl in PbS than in PbSe should be expected. Indeed, typical charge carrier concentrations with maximal self-compensation in PbS:Tl proved to be an order of magnitude lower, while the thallium concentration N_i^*, at which the sign of the charge carriers changes, was significantly higher ($N_i^* \approx 1.5$ at.%) than in PbSe:Tl [108, 109, 113]. Small values of δ in PbS are conditioned by a relatively wide forbidden band in comparison to other lead chalcogenides. This means that experimental findings are qualitatively consistent with what is expected from the theory of compensation by simple defects, which was used in interpreting the observable data for PbSe:Tl (see above, Section 6.1). The reason for the strong scatter in the experimental points for $p - n$ is also understandable: at high degrees of compensation, a modest fluctuation of parameters determining the defect concentrations proves to be sufficient for the difference concentration of charge carriers to change sharply.

A lack of adequate information about the parameters of band structure and the Tl impurity band at high temperatures hampers quantitative computation of the self-compensation in PbS:Tl. Having improved these parameters, the authors of Ref. [113] came to recognize that in explaining the self-compensation effect in PbS:Tl there is a need to invoke the complexes, especially in the range of large thallium content.

6.4 Impurity states in compensated samples of lead chalcogenides

The presence of a large amount of impurities and defects in self-compensated lead chalcogenides at relatively low charge carrier concentrations produces a series of peculiarities which were interpreted as far as the localized and quasi-local states are concerned; these states were not observed in uncompensated samples [43, 50, 110, 114].

In Ref. [114], the Hall coefficients were measured along with optical absorption in strongly self-compensated samples of lead chalcogenides and their thallium-doped solid solutions with hole concentrations $p \leqslant 10^{18}$ cm^{-3}. An observed drop in the Hall coefficient with increasing temperature was explained by a rise in the hole concentration due to thermal activation of electrons to localized levels lying above the valence-band edge by 0.05 – 0.10 eV. The presence of additional bands in the optical absorption spectra with a sharp red edge also pointed toward the existence of localized states; the 'optical' component of the localized-state energy was somewhat higher (by 0.01 – 0.02 eV) than that of the 'thermal' component. Similar temperature dependences of the Hall coefficient in thallium-doped strongly compensated n-type samples [110] have been associated at low temperatures (up to 200 K) with the ionization of donor centers located in the forbidden band 0.01 eV below the bottom of the conduction band.

The electrophysical properties of thallium-doped PbTe samples with a hole concentration of order 10^{19} cm^{-3}, which are weaker compensated for by excess lead, turned out to be different. In particular, the Hall concentration of holes was stabilized at a level of $(1.1 \pm 0.3) \times 10^{19}$ cm^{-3}, which corresponds to the chemical potential of holes equal to 0.08 eV at $T = 77$ K. The same stabilization level of the chemical potential was observed by the authors of Refs [115, 116] in epitaxial layers of PbTe:Tl grown from a lead-enriched charge. A rise of the Hall coefficient with increasing temperature was seen over a range of essentially lower temperatures (4.2 – 77 K) than in the uncompensated samples with thallium, where the temperature elevation is explained by the holes transferring to the heavy-hole band as well as to the above-discussed impurity band lying at a depth $\varepsilon_i \approx 0.2$ eV. Finally, a drastic decline in the hole mobility along with the presence of a deep minimum in the dependence of the thermo-emf on the hole concentration bear evidence to the presence of resonance scattering. Analysis of the above-listed experimental findings led the authors of Ref. [43] to the conclusion that in compensated PbTe:Tl samples there is a second band of quasi-local states over a range of hole energies of ~ 0.1 eV with a width of approximately 20 meV apart from the resonance states characterized by an energy $\varepsilon_i \approx 0.2$ eV. Similar results were also obtained in the case of $Pb_{0.95}Sn_{0.05}Te$:Tl solid solution [50]. The second quasi-local level, like the Tl level described above, became displaced deep into the valence band on substitution of tin for lead.

New local and quasi-local states discovered in compensated lead chalcogenide samples were ascribed by the authors of Refs [43, 50, 114] to complexes of intrinsic defects (vacancies) or to vacancy – impurity atom complexes. The formation of such complexes proves to be energetically favorable at high defect and impurity concentrations.

7. Conclusions

The body of experimental data outlined in the review unambiguously testifies to the existence of a wide band of resonance states deep within the valence band of thallium-doped lead chalcogenides. These states cause pinning (stabilization) of the chemical potential, resonance scattering of holes, an essential increase in the low-temperature heat capacity, the appearance of additional bands in the optical absorption spectra, superconductivity, and some other effects. The analysis of mutually coincident experimental facts provided comprehensive data on the depth of the resonance band, its dependence on temperature, pressure and the composition of the solid solution, and finally, on the bandwidth.

At the same time, questions of the genetic linkage between resonance levels and energy bands, the symmetry of impurity wave functions, the microscopic mechanism of superconductivity, the magnitude and sign of the interaction energy of electrons located at a single impurity center are still open. The resolution of these issues calls for considerable progress in the theoretical examination of group III element doping of semiconducting crystals, and in developing novel experimental procedures.

Acknowledgments

The authors are grateful to V I Kaidanov, who opened a new avenue of attack on the problem of impurities in the IV – VI compounds, for fruitful collaboration and stimulating discussions. We specially thank A N Veĭs, B A Volkov, S N Lykov, R V Parfen'ev, S A Rykov, I A Chernik, D V Shamshur, and some other researchers who significantly contributed to the investigation of the effects of thallium dopant on semiconducting materials.

References

1. Averkin A A, Kaĭdanov V I, Mel'nik R B *Fiz. Tekh. Poluprovodn.* **5** 91 (1971)
2. Kaĭdanov V I, Mel'nik R B, Chernik I A *Fiz. Tekh. Poluprovodn.* **7** 759 (1973)
3. Kaĭdanov V I, Ravich Yu I *Usp. Fiz. Nauk* **145** 51 (1985) [*Sov. Phys. Usp.* **28** 31 (1985)]
4. Lykov S N, Chernik I A *Fiz. Tekh. Poluprovodn.* **14** 47 (1980) [*Sov. Phys. Semicond.* **14** 25 (1980)]
5. Veĭs A N et al. *Fiz. Tekh. Poluprovodn.* **11** 699 (1977) [*Sov. Phys. Semicond.* **11** 409 (1977)]
6. Veĭs A N et al. *Fiz. Tekh. Poluprovodn.* **13** 185 (1979) [*Sov. Phys. Semicond.* **13** 106 (1979)]
7. Kaĭdanov V I, Mel'nik R B, Nemov S A *Fiz. Tekh. Poluprovodn.* **13** 1011 (1979) [*Sov. Phys. Semicond.* **13** 591 (1979)]
8. Kaĭdanov V I, Nemov S A, Ravich Yu I *Fiz. Tekh. Poluprovodn.* **26** 201 (1992) [*Sov. Phys. Semicond.* **26** 113 (1992)]
9. Akimov B A et al. *Pis'ma Zh. Eksp. Teor. Fiz.* **29** 11 (1979) [*JETP Lett.* **29** 9 (1979)]
10. Vul B M et al. *Pis'ma Zh. Eksp. Teor. Fiz.* **29** 21 (1979) [*JETP Lett.* **29** 18 (1979)]
11. Volkov B A, Osipov V V, Pankratov O A *Fiz. Tekh. Poluprovodn.* **14** 1387 (1980) [*Sov. Phys. Semicond.* **14** 820 (1980)]
12. Volkov B A, Pankratov O A *Dokl. Akad. Nauk SSSR* **255** 93 (1980) [*Sov. Phys. Doklady* **25** 922 (1980)]
13. Andreev Yu V et al. *Fiz. Tekh. Poluprovodn.* **9** 1873 (1975) [*Sov. Phys. Semicond.* **9** 1235 (1975)]
14. Moĭzhes B Ya, Drabkin I A, in *Problemy sovremennoĭ fiziki. Sbornik stateĭ k 100-letiyu so dnya rozhdeniya A F Ioffe* (Problems of Modern Physics) (Leningrad: Nauka, 1980) p. 128
15. Drabkin I A, Moizhes B Ya *Fiz. Tekh. Poluprovodn.* **15** 625 (1981) [*Sov. Phys. Semicond.* **15** 357 (1981)]
16. Anderson P W *Phys. Rev. Lett.* **34** 953 (1975)
17. Lykov S N, Ravich Yu I, Chernik I A *Fiz. Tekh. Poluprovodn.* **11** 1731 (1977) [*Sov. Phys. Semicond.* **11** 1016 (1977)]
18. Nemov S A et al. *Fiz. Tekh. Poluprovodn.* **27** 299 (1993) [*Semicond.* **27** 165 (1993)]
19. Ravich Yu I, Nemov S A, Proshin V I *Fiz. Tekh. Poluprovodn.* **29** 1448 (1995) [*Semicond.* **29** 754 (1995)]
20. Ravich Yu I, Efimova B A, Smirnov I A *Semiconducting Lead Chalcogenides* (New York: Plenum, 1970) [Translated from Russian *Metody issledovaniya poluprovodnikov v primenenii k khal'kogenidam svintsa PbTe, PbSe i Pb-S* (Moscow: Nauka, 1968)]
21. Dornhaus R, Nimtz G, Schlicht B *Narrow-Gap Semiconductors* (Springer Tracts in Modern Physics, 98) (Berlin, New York: Springer, 1983)
22. *Landolt-Börnstein. Numerical Data and Functional Relationships in Science and Technology*, New series, Group III, Vol. 17, subvol. f (Berlin: Springer, 1983)
23. Volkov B A, Pankratov O A *Zh. Eksp. Teor. Fiz.* **75** 1362 (1978) [*Sov. Phys. JETP* **48** 687 (1978)]
24. Volkov B A, Pankratov O A, Sazonov A V *Fiz. Tekh. Poluprovodn.* **16** 1734 (1982) [*Sov. Phys. Semicond.* **16** 1112 (1982)]
25. Volkov B A, Pankratov O A, Sazonov A V *Zh. Eksp. Teor. Fiz.* **85** 1395 (1983) [*Sov. Phys. JETP* **58** 809 (1983)]
26. Ravich Yu I, Efimova B A, Tamarchenko V I *Phys. Status Solidi B* **43** 11, 453 (1971)
27. Herman F, Skillman S *Atomic Structure Calculations* (Englewood Cliffs, N.J.: Prentice-Hall, 1963)
28. Veĭs A N et al. *Fiz. Tekh. Poluprovodn.* **11** 995 (1977) [*Sov. Phys. Semicond.* **11** 588 (1977)]
29. Kaĭdanov V I et al. *Fiz. Tekh. Poluprovodn.* **11** 1187 (1977) [*Sov. Phys. Semicond.* **11** 701 (1977)]
30. Veĭs A N, Kaĭdanov V I, Nemov S A *Fiz. Tekh. Poluprovodn.* **12** 1599 (1978) [*Sov. Phys. Semicond.* **12** 943 (1978)]
31. Gotuk A A, Babanly M B, Kuliev A A *Izv. Akad. Nauk SSSR, Ser. Neorg. Mater.* **14** 587 (1978)
32. Mashkova T R, Nemov S A *Fiz. Tekh. Poluprovodn.* **19** 1864 (1985) [*Sov. Phys. Semicond.* **19** 1148 (1985)]
33. Veĭs A N, Kaĭdanov V I, Nemov S A *Fiz. Tekh. Poluprovodn.* **14** 1054 (1980) [*Sov. Phys. Semicond.* **14** 628 (1980)]
34. Veĭs A N, Kaĭdanov V I, Nemov S A *Fiz. Tekh. Poluprovodn.* **17** 1948 (1983) [*Sov. Phys. Semicond.* **17** 1245 (1983)]
35. Kaĭdanov V I, Nemov S A, Zaĭtsev A M *Fiz. Tekh. Poluprovodn.* **19** 268 (1985) [*Sov. Phys. Semicond.* **19** 165 (1985)]
36. Kaz'min S A et al. *Fiz. Tverd. Tela* **26** 3205 (1984) [*Sov. Phys. Solid State* **26** 1930 (1984)]
37. Kaĭdanov V I et al. *Pis'ma Zh. Eksp. Teor. Fiz.* **35** 517 (1982) [*JETP Lett.* **35** 639 (1982)]
38. Kaĭdanov V I et al. *Fiz. Tekh. Poluprovodn.* **17** 1613 (1983) [*Sov. Phys. Semicond.* **17** 1027 (1983)]
39. Kaĭdanov V I et al. *Fiz. Tekh. Poluprovodn.* **18** 1288 (1984) [*Sov. Phys. Semicond.* **18** 804 (1984)]
40. Nemov S A, Ravich Yu I, Zaĭtsev A M *Fiz. Tekh. Poluprovodn.* **19** 636 (1985) [*Sov. Phys. Semicond.* **19** 393 (1985)]
41. Kaĭdanov V I et al. *Fiz. Tverd. Tela* **29** 1886 (1987) [*Sov. Phys. Solid State* **29** 1086 (1987)]
42. Gartsman K G, Zhukova T B, Nemov S A *Izv. Akad Nauk SSSR, Ser. Neorg. Mater.* **21** 498 (1985)
43. Kaĭdanov V I et al. *Fiz. Tekh. Poluprovodn.* **20** 859 (1986) [*Sov. Phys. Semicond.* **20** 541 (1986)]
44. Abaĭdulina T G et al. *Fiz. Tekh. Poluprovodn.* **30** 2173 (1996) [*Semicond.* **30** 1133 (1996)]
45. Nemov S A et al. *Fiz. Tverd. Tela* **38** 550 (1996) [*Phys. Solid. State* **38** 301 (1996)]
46. Nemov S A et al. *Fiz. Tverd. Tela* **38** 1586 (1996) [*Phys. Solid State* **38** 872 (1996)]
47. Masterov V F, Zakharenkov L F *Fiz. Tekh. Poluprovodn.* **24** 610 (1990) [*Sov. Phys. Semicond.* **24** 383 (1990)]
48. Tsidil'kovskiĭ I M *Fiz. Tekh. Poluprovodn.* **24** 593 (1990) [*Sov. Phys. Semicond.* **24** 373 (1990)]
49. Kaĭdanov V I, Nemov S A *Fiz. Tekh. Poluprovodn.* **15** 542 (1981) [*Sov. Phys. Semicond.* **15** 306 (1981)]
50. Nemov S A, Bogatyrenko N G, Proshin V I *Fiz. Tekh. Poluprovodn.* **24** 1391 (1990) [*Sov. Phys. Semicond.* **24** 873 (1990)]
51. Nemov S A, Ravich Yu I *Fiz. Tekh. Poluprovodn.* **22** 1370 (1988) [*Sov. Phys. Semicond.* **22** 869 (1988)]
52. Chernik I A, Lykov S N *Fiz. Tverd. Tela* **23** 2956 (1981) [*Sov. Phys. Solid State* **23** 1724 (1981)]
53. Herring C *J. Appl. Phys.* **31** 1939 (1960)
54. Boĭko M P et al. *Fiz. Tekh. Poluprovodn.* **21** 1303 (1987) [*Sov. Phys. Semicond.* **21** 791 (1987)]
55. Kaĭdanov V I et al. *Fiz. Tverd. Tela* **28** 1058 (1986) [*Sov. Phys. Solid State* **28** 591 (1986)]
56. Borovikova R P et al. *Izv. Akad. Nauk SSSR, Neorg. Mater.* **12** 1749 (1976)
57. Chernik I A *Fiz. Tekh. Poluprovodn.* **14** 80 (1980) [*Sov. Phys. Semicond.* **14** 44 (1980)]
58. Bushmarina G S et al. *Fiz. Tekh. Poluprovodn.* **18** 2203 (1984) [*Sov. Phys. Semicond.* **18** 1374 (1984)]
59. Kaĭdanov V I et al. *Fiz. Tekh. Poluprovodn.* **20** 1102 (1986) [*Sov. Phys. Semicond.* **20** 693 (1986)]
60. Ravich Yu I, in *CRC Handbook of Thermoelectrics* (Ed. D M Rowe) (Boca Raton, FL: CRC Press, 1995) p. 67
61. Andronik K I et al. *Phys. Status Solidi B* **133** K61 (1986)
62. Andronik K I et al., in *Polumetally i Uzkozonnye Poluprovodniki* (Semi-metals and Narrow-Gap Semiconductors) (Ed. D V Gitsu)(Kishinev: Shtiintsa, 1988) p. 129
63. Kondo J *Prog. Theor. Phys.* **32** 37 (1964)
64. Ootuka Y et al. *Solid State Commun.* **30** 169 (1979)
65. Anderson P W *Phys. Rev.* **124** 41 (1961)
66. Andronik K I, Boĭko M P, Luzhkovskiĭ A V *Fiz. Tekh. Poluprovodn.* **22** 1878 (1988) [*Sov. Phys. Semicond.* **22** 1190 (1988)]
67. Veĭs A N, Nemov S A *Izv. Vyssh. Uchebn. Zaved., Ser. Fiz.* **25** (7) 113 (1982)
68. Veĭs A N, Kaĭdanov V I, Krupitskaya R Yu *Fiz. Tekh. Poluprovodn.* **22** 349 (1988) [*Sov. Phys. Semicond.* **22** 215 (1988)]
69. Andronik K I, *Thesis for Candidate of Physicomathematical Sciences* (Kishinev, 1990)
70. Baginskiĭ V M et al., in *Poluprovodniki s Uzkoĭ Zapreshchennoĭ Zonoĭ i Polumetally* (Narrow-Gap Semiconductors and Semimetals)(Proc. IV All-Union Symp., Part III)(L'vov: Visha Shkola, 1975) p. 51

71. Chernik I A, Berezin A V, Lykov S N *Fiz. Tverd. Tela* **32** 947 (1990) [*Sov. Phys. Solid State* **32** 560 (1990)]
72. Chernik I A et al. *Fiz. Tverd. Tela* **34** 2454 (1992) [*Sov. Phys. Solid State* **34** 1316 (1992)]
73. Ravich Yu I, Chernik I A, Berezin A V *Fiz. Tverd. Tela* **34** 2537 (1992) [*Sov. Phys. Solid State* **34** 1360 (1992)]
74. Veĭs A N, Nemov S A *Fiz. Tekh. Poluprovodn.* **13** 2384 (1979) [*Sov. Phys. Semicond.* **13** 1394 (1979)]
75. Veĭs A N, Nemov S A *Fiz. Tekh. Poluprovodn.* **15** 1237 (1981) [*Sov. Phys. Semicond.* **15** 715 (1981)]
76. Veĭs A N *Fiz. Tekh. Poluprovodn.* **21** 263 (1987) [*Sov. Phys. Semicond.* **21** 159 (1987)]
77. Veĭs A N, Krupitskaya R Yu *Fiz. Tekh. Poluprovodn.* **23** 185 (1989) [*Sov. Phys. Semicond.* **23** 117 (1989)]
78. Veĭs A N *Fiz. Tekh. Poluprovodn.* **25** 1934 (1991) [*Sov. Phys. Semicond.* **25** 1165 (1991)]
79. Konstantinov P P et al. *Fiz. Tverd. Tela* **24** 3530 (1982) [*Sov. Phys. Solid State* **24** 2011 (1982)]
80. Kaĭdanov V I, Rykov S A, Rykova M A *Fiz. Tverd. Tela* **31** (8) 68 (1989) [*Sov. Phys. Solid State* **31** 1316 (1989)]
81. Kaĭdanov V I et al. *Fiz. Tekh. Poluprovodn.* **24** 144 (1990) [*Sov. Phys. Semicond.* **24** 87 (1990)]
82. Chernik I A, Lykov S N *Pis'ma Zh. Tekh. Fiz.* **7** 94 (1981) [*Tech. Phys. Lett.* **7** 40 (1981)]
83. Chernik I A, Lykov S N *Fiz. Tverd. Tela* **23** 1400 (1981) [*Sov. Phys. Solid State* **23** 817 (1981)]
84. Chernik I A, Lykov S N *Fiz. Tverd. Tela* **23** 3548 (1981) [*Sov. Phys. Solid State* **23** 2062 (1981)]
85. Kaz'min S A et al. *Fiz. Tverd. Tela* **24** 1462 (1982) [*Sov. Phys. Solid State* **24** 832 (1982)]
86. Lalevic B *Phys. Lett.* **16** 206 (1965)
87. Lasbley A, Granger R, Rolland S *Solid State Commun.* **13** 1045 (1973)
88. Johnson A C et al. *Solid State Commun.* **16** 803 (1975)
89. Zhitinskaya M K, Kaĭdanov V I, Lykov S N *Fiz. Tekh. Poluprovodn.* **13** 183 (1979) [*Sov. Phys. Semicond.* **13** 105 (1979)]
90. Buckel W *Supraleitung Grundlagen und Anwendungen* (Weinheim: Bergser, 1972) [Translated into Russian (Moscow: Mir, 1975)] [Translated into English (Super–Conductivity) (Weinheim, New York: VCH, 1991)]
91. Lifshitz E M, Pitaevskiĭ L P *Statistical Physics* Part 2 (Oxford: Pergamon Press, 1980)
92. Bushmarina G S et al. *Fiz. Tverd. Tela* **28** 1094 (1986) [*Sov. Phys. Solid State* **28** 612 (1986)]
93. Chernik I A, Lykov S N, Grechko N I *Fiz. Tverd. Tela* **24** 2931 (1982) [*Sov. Phys. Solid State* **24** 1661 (1982)]
94. Ting C S, Talwar D N, Ngai K L *Phys. Rev. Lett.* **45** 1213 (1980)
95. Kulik I O, Pedan A G *Zh. Eksp. Teor. Fiz.* **79** 1469 (1980) [*Sov. Phys. JETP* **52** 742 (1980)]
96. Moĭzhes B Ya *Pis'ma Zh. Tekh. Fiz.* **7** 570 (1981) [*Tech. Phys. Lett.* **7** 244 (1981)]
97. Moĭzhes B Ya, Suprun S G *Fiz. Tverd. Tela* **27** 1395 (1985) [*Sov. Phys. Solid State* **27** 842 (1985)]
98. Moĭzhes B Ya, Suprun S G *Fiz. Tverd. Tela* **29** 441 (1987) [*Sov. Phys. Solid State* **29** 252 (1987)]
99. Volkov B A, Tugushev V V *Pis'ma Zh. Eksp. Teor. Fiz.* **46** 193 (1987) [*JETP Lett.* **46** 245 (1987)]
100. Nemov S A, Parfen'ev R V, Shamshur D V *Fiz. Tverd. Tela* **27** 589 (1985) [*Sov. Phys. Solid State* **27** 368 (1985)]
101. Erasova N A, Lykov S N, Chernik I A *Fiz. Tverd. Tela* **25** 269 (1983) [*Sov. Phys. Solid State* **25** 150 (1983)]
102. Zhitinskaya M K et al. *Fiz. Tverd. Tela* **31** 268 (1989) [*Sov. Phys. Solid State* **31** 701 (1989)]
103. Kaĭdanov V I et al. *Fiz. Tverd. Tela* **27** 2513 (1985) [*Sov. Phys. Solid State* **27** 1506 (1985)]
104. Zhitinskaya M K et al. *Fiz. Tverd. Tela* **32** 122 (1990) [*Sov. Phys. Solid State* **32** 67 (1990)]
105. Abdullin Kh A et al. *Pis'ma Zh. Eksp. Teor. Fiz.* **40** 229 (1984) [*JETP Lett.* **40** 998 (1984)]
106. Mandel G *Phys. Rev.* **134** A1073 (1964)
107. Vinetskiĭ V L, Kholodar' G A *Statisticheskoe Vzaimodeistvie Elektronov i Defektov v Poluprovodnikakh* (Statistical Interaction of Electrons and Defects in Semiconductors) (Kiev: Naukova Dumka, 1969)
108. Bytenskiĭ L I et al. *Fiz. Tekh. Poluprovodn.* **14** 74 1980) [*Sov. Phys. Semicond.* **14** 40 (1980)]
109. Kaĭdanov V I, Nemov S A, Ravich Yu I *Fiz. Tekh. Poluprovodn.* **28** 369 (1994) [*Semicond.* **28** 223 (1994)]
110. Zhitinskaya M K et al. *Fiz. Tekh. Poluprovodn.* **22** 2043 (1988) [*Sov. Phys. Semicond.* **22** 1292 (1988)]
111. Bytenskiĭ L I et al. *Fiz. Tekh. Poluprovodn.* **15** 981 (1981) [*Sov. Phys. Semicond.* **15** 563 (1981)]
112. Bytenskiĭ L I et al. *Fiz. Tekh. Poluprovodn.* **18** 489 (1984) [*Sov. Phys. Semicond.* **18** 303 (1984)]
113. Erasova N A et al. *Fiz. Tekh. Poluprovodn.* **21** 2210 (1987) [*Sov. Phys. Semicond.* **21** 1339 (1987)]
114. Veĭs A N et al. *Fiz. Tekh. Poluprovodn.* **14** 2349 (1980) [*Sov. Phys. Semicond.* **14** 1392 (1980)]
115. Feit Z, Zemel A, Eger D, Sternberg I, in *Proc. 4th Int. Conf. Phys. Narrow-Gap Semiconductors., Linz, Austria, 1982* (Berlin, New York: Springer, 1982) p. 69
116. Feit Z, Eger D, Zemel A *Phys. Rev. B* **31** 3903 (1985)